

ND-A168 575

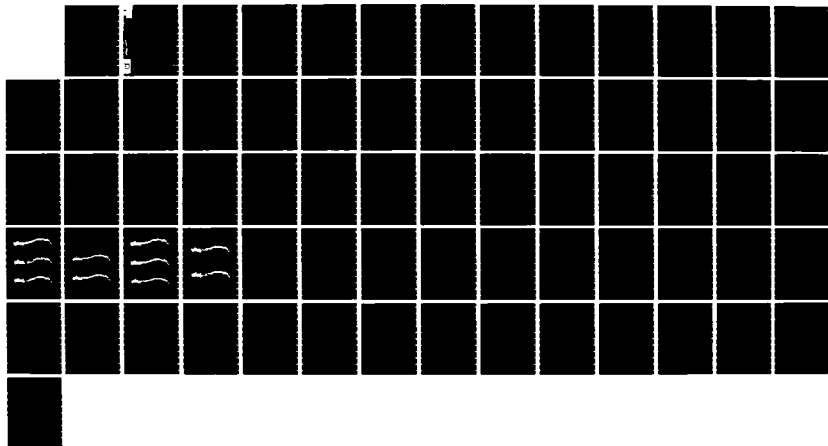
DEVELOPMENT OF AN ADAPTIVE BOUNDARY-FITTED COORDINATE
CODE FOR USE IN COA.. (U) ARMY ENGINEER WATERWAYS
EXPERIMENT STATION VICKSBURG MS HYDRA.

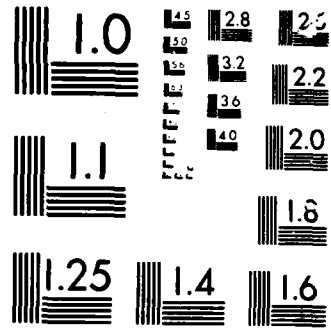
2/1

UNCLASSIFIED

J F THOMPSON ET AL. SEP 85 WES/MP/HL-85-5 F/G 8/3

NL

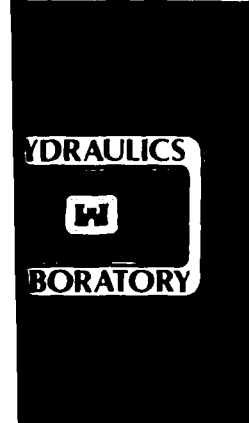
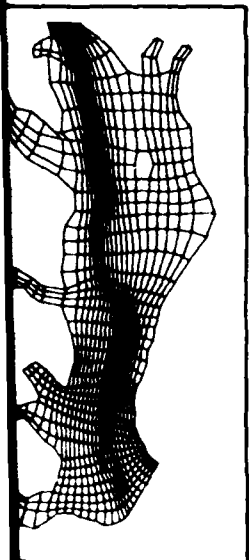






U.S. Army Corps
Engineers

AD-A168 575



MISCELLANEOUS PAPER HL-85-5

(2)

DEVELOPMENT OF AN ADAPTIVE BOUNDARY-FITTED COORDINATE CODE FOR USE IN COASTAL AND ESTUARINE AREAS

by

Joe F. Thompson, Billy H. Johnson

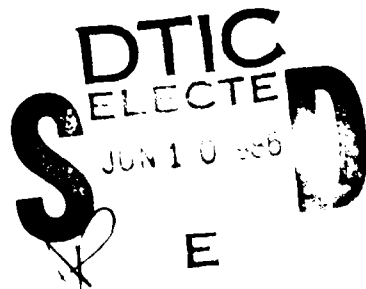
Hydraulics Laboratory

DEPARTMENT OF THE ARMY
Waterways Experiment Station, Corps of Engineers
PO Box 631, Vicksburg, Mississippi 39180-0631



September 1985
Final Report

Approved For Public Release. Distribution Unlimited



Prepared for DEPARTMENT OF THE ARMY
Assistant Secretary of the Army (R&D)
Washington, DC 20315

DTIC FILE COPY Under Project No. 4A061101A91D

86 6 10 108

Destroy this report when no longer needed. Do not return
it to the originator.

The findings in this report are not to be construed as an official
Department of the Army position unless so designated
by other authorized documents.

The contents of this report are not to be used for
advertising, publication, or promotional purposes.
Citation of trade names does not constitute an
official endorsement or approval of the use of
such commercial products.

Unclassified

SECURITY CLASSIFICATION OF THIS PAGE (When Data Entered)

REPORT DOCUMENTATION PAGE		READ INSTRUCTIONS BEFORE COMPLETING FORM
1. REPORT NUMBER Miscellaneous Paper HL-85-5	2. GOVT ACCESSION NO. ADA 168575	3. RECIPIENT'S CATALOG NUMBER
4. TITLE (and Subtitle) DEVELOPMENT OF AN ADAPTIVE BOUNDARY-FITTED COORDINATE CODE FOR USE IN COASTAL AND ESTUARINE AREAS	5. TYPE OF REPORT & PERIOD COVERED Final report	
7. AUTHOR(s) Joe F. Thompson Billy H. Johnson	6. PERFORMING ORG. REPORT NUMBER	
9. PERFORMING ORGANIZATION NAME AND ADDRESS US Army Engineer Waterways Experiment Station Hydraulics Laboratory PO Box 631, Vicksburg, Mississippi 39180-0631	10. PROGRAM ELEMENT, PROJECT, TASK AREA & WORK UNIT NUMBER Project 4A061101A91D	
11. CONTROLLING OFFICE NAME AND ADDRESS DEPARTMENT OF THE ARMY Assistant Secretary of the Army (R&D) Washington, DC 20314-0001	12. REPORT DATE September 1985	
14. MONITORING AGENCY NAME & ADDRESS (if different from Controlling Office)	13. NUMBER OF PAGES 64	
15. SECURITY CLASS (of this report) Unclassified		
15a. DECLASSIFICATION/DOWNGRADING SCHEDULE		
16. DISTRIBUTION STATEMENT (of this Report) Approved for public release; distribution unlimited.		
17. DISTRIBUTION STATEMENT (of the abstract entered in Block 20, if different from Report)		
18. SUPPLEMENTARY NOTES Available from National Technical Information Service, 5285 Port Royal Road, Springfield, Virginia 22161.		
19. KEY WORDS (Continue on reverse side if necessary and identify by block number) Chesapeake Bay (Md. and Va.) (LC) Harbors--Hydrodynamics--Mathematical models (LC) Two dimensional flow (WES) WESCORA (computer program) (LC)		
20. ABSTRACT (Continue on reverse side if necessary and identify by block number) Most coastal and estuarine systems that have problems requiring numerical hydrodynamic and transport modeling contain winding navigation channels. Accurate and efficient modeling of flow and suspended sediment transport requires a numerical grid that follows the navigation channel with a fine grid spacing in the channel, while retaining a larger spacing in the remainder of the field. A computer program called WESCORA has been developed to enable the numerical		
(Continued)		

Unclassified

SECURITY CLASSIFICATION: THIS PAGE (When Data Entered)

20. ABSTRACT (Continued).

computation of such boundary-fitted grids for use in the finite difference modeling of flow and constituent fields.

Two adaption mechanisms are included, one based on a variational principle and the other based on control functions, with the former being apparently the more consistent and reliable. With the variational approach, a functional that consists of the sum of three integrals involving the physical coordinates is minimized over the grid. The first of the integrals controls grid point concentration by forcing the grid points to cluster where the water depth is large, i.e., in navigation channels. The other two integrals control grid smoothness, i.e., the rate of change of grid spacing and the skewness of the coordinate lines. By weighting the importance of the three integrals, either grid point concentration, grid smoothness, or orthogonality can be emphasized.

Mathematical aspects of the grid generation equations and the interpolation schemes employed for the water depths are discussed. In addition, example grids generated on Chesapeake Bay are presented.

Unclassified

SECURITY CLASSIFICATION OF THIS PAGE (When Data Entered)

PREFACE

The study reported herein was conducted during the period February 1985 to September 1985 by the Hydraulics Laboratory of the US Army Engineer Waterways Experiment Station (WES) under the general supervision of Messrs. F. A. Herrmann, Jr., Chief of the Hydraulic Laboratory, and M. B. Boyd, Chief of the Hydraulics Analysis Division (HAD). The study was funded by Department of the Army Project 4A061101A91D, "In-House Laboratory Independent Research," sponsored by the Assistant Secretary of the Army.

Dr. B. H. Johnson, HAD, directed the study and jointly prepared the report with the coauthor Dr. J. F. Thompson of the Department of Aerospace Engineering at Mississippi State University. This report was edited by Mrs. Beth F. Vavra, Publications and Graphic Arts Division.

Director of WES was COL Allen F. Grum, USA. Technical Director was Dr. Robert W. Whalin.

Accession For	
NTIS	DTIC
DTIC	<input checked="" type="checkbox"/>
Uni	<input type="checkbox"/>
J	<input type="checkbox"/>
F	
P	
S	
T	

A1



CONTENTS

	<u>Page</u>
PREFACE	1
PART I: INTRODUCTION	3
Numerical Techniques	3
Boundary-Fitted Coordinates Concept	4
WESCOR	4
Need for a New Grid Generator	5
PART II: ADAPTIVE GRIDS	7
Variational Formulation	7
Control Function Formulation	11
PART III: DEPTH INTERPOLATION	13
Taylor Series Expansion About Nearest Depth Point	13
Interpolation Within Triangles or Quadrilaterals of Depth Points	14
Inverse-Power Interpolation Among Depth Points	15
Location of Neighboring Depth Points	15
PART IV: GENERATION PROCEDURE	21
Iterative Solution	21
Weight Function	21
Input	22
PART V: CHESAPEAKE BAY APPLICATION	25
Chesapeake Bay	25
Selection of Boundary Points	25
Grid Generation Using Actual Depths	26
Grid Generation Using Hypothetical Depths	26
Influence of Weighting Factors	27
Practical Aspects	27
PART VI: SUMMARY AND CONCLUSIONS	29
Summary	29
Conclusions	29
REFERENCES	31
FIGURES 1-17	
TABLE 1	
APPENDIX A: INPUT INSTRUCTIONS	A1
APPENDIX B: CYBERNET JOB STREAMS AND EXAMPLE INPUT FOR CHESAPEAKE BAY	B1

DEVELOPMENT OF AN ADAPTIVE BOUNDARY-FITTED COORDINATE CODE
FOR USE IN COASTAL AND ESTUARINE AREAS

PART I: INTRODUCTION

1. The mathematical modeling of the hydrodynamics of a body of water plus the transport and dispersion of a constituent within that body involves the solution of a set of partial differential equations expressing the conservation of mass, momentum, and energy of the flow field along with a transport equation for the constituent. These equations involve derivatives with respect to time as well as three spatial dimensions. However, a simplification that is often made in treating relatively shallow bodies of water which are well mixed over the depth is to vertically average the three-dimensional (3-D) equations to yield a two-dimensional (2-D) set for nearly horizontal flows.

Numerical Techniques

2. Since the governing equations are nonlinear, analytic solutions in general cannot be found and one is forced to resort to numerical techniques to obtain solutions. The two most common such techniques are the finite difference method (FDM) and the finite element method (FEM). There are, of course, both advantages and disadvantages to each of these approaches.

3. Perhaps the most often quoted advantage of the FEM is that with this approach, physical boundaries coincide with computational net points. Therefore the modeling of flow within an irregular domain can be more accurately handled than with the older rectangular FDM wherein the approach is to construct a rectangular grid over the domain, which forces the boundaries to be represented in a "stair-stepped" fashion. However, a disadvantage of many finite element models is the excessive computational time required compared with typical finite difference models having the same number of mesh points. As discussed by Johnson, Thompson, and Baker (1984) this occurs because of the manner in which the system of resulting algebraic equations is usually solved in finite element models. An additional disadvantage is that the FEM is more cumbersome to code into a computer model than the FDM. This can be a problem not only during the development of the model but also can increase the level of effort required during later model modifications.

Boundary-Fitted Coordinates Concept

4. Accepting that the FDM possesses an advantage in simplicity and perhaps computational costs, a logical question is whether or not one can develop ways to circumvent the major disadvantage of having to represent irregular boundaries in a stair-stepped fashion. One method is to make computations on curvilinear grids so that one of the curvilinear coordinates always follows a boundary. Vertically averaged hydrodynamic models developed by Johnson (1980) and Sheng and Hirsh (1984) are examples of models employing a general non-orthogonal curvilinear grid. Through coordinate transformations, irregular boundaries and variable grid spacing can be more accurately handled while still making use of the simplicity of finite differences to obtain solutions. Since the boundary-fitted coordinate system has a coordinate line coincident with all boundaries, all boundary conditions can be expressed at grid points; and normal derivatives can be represented using only finite differences between grid points on coordinate lines. No interpolation is needed, even though the coordinate system is not orthogonal at the boundary. A general discussion is given by Thompson, Warsi, and Mastin (1985).

5. To enable efficient flow-transport modeling on boundary-fitted grids, a numerical generator is needed to provide the (x,y) location of the curvilinear coordinates. One of the earliest grid generators was developed by Thompson, Thames, and Mastin (1977) with a later version called WESCOR provided by Thompson (1983).

WESCOR

6. The WESCOR code generates a boundary-conforming curvilinear coordinate system for a general 2-D region with boundaries of arbitrary shape and with boundary intrusions and internal obstacles, such as islands, arbitrary in shape and number. The grid is generated from the numerical solution of a set of elliptic partial differential equations by accelerated point Gauss-Seidel iteration.

7. These equations are written in the transformed space, which is inherently rectangular with a square grid. All computations, both to generate the grid and subsequently to solve partial differential equations for physical problems on the grid, are done in this transformed space, so that all boundary

conditions can be represented on grid lines without interpolation. This allows codes to be constructed that treat completely arbitrary regions with rectangular DO loops, with the boundary shape specified simply by an input boundary point distribution. It is thus possible to treat arbitrary boundary shapes naturally with FDM's, although such grids can also serve in finite element solutions.

8. The WESCOR code incorporates an automatic evaluation of two control functions in the elliptic generation system from the specified boundary point distribution that serves to make the grid lines in the field follow the general relative distribution of points on the boundaries. The code also allows for this automatic grid line control to be augmented by input to concentrate grid lines near other grid lines and/or points.

Need for a New Grid Generator

9. As noted, much of the numerical modeling of free-surface hydrodynamics involves the depth-averaged computation of circulation patterns in estuaries and coastal areas to provide input to numerical transport-diffusion models of sediment and water quality parameters. In many of these problems a major concern is the representation of winding navigation channels on the numerical grid. Existing boundary-fitted grid generation codes, e.g. WESCOR, cannot generate adequate grids for such problems, thus a grid generation code that forces grid points to cluster along an internal navigation channel is required before finite difference models based upon boundary-fitted coordinates can be efficiently applied to coastal and estuarine areas. In a recent study by Johnson, Thompson, and Baker (1984) it was recommended that an estuarine/coastal fixed-grid generator model based upon adaptive grid techniques be developed.

10. To accomplish this, the 2-D numerical grid generation code WESCOR has been extended to include adaption of the grid to concentrate lines according to a depth distribution. The present extension automatically concentrates grid lines according to increasing depth. Two adaption mechanisms are included, one based on the variational formulation of Brackbill and Saltzman (1982) that uses the calculus of variations to produce a system of partial differential equations with competitive enhancement of grid concentration, smoothness, and orthogonality, and the other based on a simple

extension of the control functions in the original elliptic generation in WESCOR.

11. With either adaptive mechanism the code first generates a grid using the original WESCOR system without regard to depths. The input depth distribution, which is specified by an arbitrary arrangement of points with no order or pattern, is then interpolated onto this initial grid. No further interpolation is needed as the adaptive grid generation system is solved for a grid that is concentrated according to increasing depth.

12. In the following sections, discussion of the theory of the adaption mechanism, the interpolation procedures, input required, and finally an example application are presented. User instructions and sample job streams are presented in the appendices.

PART II: ADAPTIVE GRIDS

13. The generation of adaptive grids is discussed in detail by Thompson, Warsi, and Mastin (1985) and a recent survey is given by Thompson (1985). A discussion of potential applications in numerical hydrodynamic modeling is given by Johnson, Thompson, and Baker (1984). Briefly, an adaptive grid senses gradients of some physical quantity and adjusts itself automatically to better resolve those gradients, i.e., to concentrate lines in the high gradient regions. (The adaption here is through movement of the grid points, not the addition of more points.)

14. With the time derivatives at fixed values of the physical coordinates transformed to time derivatives taken at fixed values of the curvilinear coordinates, no interpolation is required when the adaptive grid moves. The time derivative transforms as follows:

$$\left(\frac{\partial u}{\partial t}\right)_{\xi, \eta} = \left(\frac{\partial u}{\partial t}\right)_{x, y} + \frac{\partial u}{\partial x} \dot{x} + \frac{\partial u}{\partial y} \dot{y} \quad (1)$$

where \dot{x}, \dot{y} are the components of the grid speed. The computation thus can be done on a fixed grid in the transformed space, without need of interpolation, even though the grid points are in motion in physical space. The influence of the motion of the grid points is registered through the grid speed appearing in the transformed time derivative.

15. Several considerations are involved here, some of which are conflicting. The points must concentrate, and yet no region can be allowed to become devoid of points. The distribution also must retain a sufficient degree of smoothness, and the grid must not become too skewed, else the truncation error of equations solved on the grid will be increased. This means that points must not move independently, but rather each point must somehow be coupled at least to its neighbors. Also, the grid points must not move too far or too fast, else oscillations may occur.

Variational Formulation

16. Thus, on the one hand, there is a need to force grid points to concentrate near large solution gradients; on the other hand, there is a need to generate grids that are relatively smooth and do not deviate too much from

being orthogonal. The calculus of variations is well suited to handle such problems since integrals over the grid can be written that measure the three desired features discussed above, namely, (a) a concentration of grid points near large solution gradients, (b) a smooth distribution of grid points, and (c) a relatively orthogonal grid. The variational formulation of adaptive grids is discussed in detail by Brackbill and Saltzman (1982) and by Thompson, Warsi, and Mastin (1985). A brief discussion follows.

17. The area of a computational cell in two dimensions (the volume in three dimensions) is given by the Jacobian, J , of the mapping:

$$J = x_\xi y_\eta - x_\eta y_\xi \quad (2)$$

Therefore, if the integral

$$I_w = \int_D w(x,y) J \, dA, \quad (3)$$

which is a measure of the weighted variation of the computational cell size over the grid, is minimized for some weight function $w(x,y)$, which is related to the solution gradient, a concentration of grid points in high gradient regions can be obtained. In other words, where the weight function $w(x,y)$ becomes large the cell size becomes small, and where $w(x,y)$ becomes small the size of the computational cell becomes large.

18. Likewise, the smoothness of the grid is measured by the integral

$$I_s = \int_D [(\nabla \xi)^2 + (\nabla \eta)^2] \, dA \quad (4)$$

with the orthogonality measured by

$$I_o = \int_D (\nabla \xi \cdot \nabla \eta)^2 J^3 \, dA \quad (5)$$

where the J^3 is added to cause orthogonality to be emphasized more in larger cells. Note that $\nabla \xi \cdot \nabla \eta = 0$ for an orthogonal grid. Therefore an adaptive grid generator can be developed by minimizing a sum of the three integrals given in Equations 3-5, i.e.,

$$I = \lambda_s I_s + \lambda_o I_o + \lambda_w I_w \quad (6)$$

19. From the above expressions for I_s , I_o , and I_w we have the dimensional relations

$$I_s \sim \frac{N^2}{L^2} L^2 ; \quad I_o \sim \frac{N^4}{L^4} \frac{L^6}{N^6} L^2 ; \quad I_w \sim W \frac{L^2}{N^2} L^2$$

where

N = characteristic number of points

L = characteristic length

W = average weight function over the field

$$W = \frac{1}{A} \int_D w(x,y) dA \quad (7)$$

Thus, for Equation 6 to be dimensionally correct, we take

$$\lambda_o = \lambda'_o \left(\frac{N}{L}\right)^4 \quad \text{and} \quad \lambda_w = \lambda'_w \left(\frac{N}{L}\right)^4 \frac{1}{W}$$

where λ'_o and λ'_w are positive constants. The characteristic length and number of points might logically be taken as the square roots of the total area and the total number of points in the field, respectively.

20. Obviously, by selecting appropriate values of λ_s , λ'_w , and λ'_o , grids that emphasize smoothness, concentration of grid points, or orthogonality can be generated. The variational formulation thus provides a competitive enhancement of these three grid characteristics. A note of caution concerning orthogonality is perhaps needed. Purely orthogonal grids cannot be generated when prescribing the location of boundary points, even if the condition $\nabla \xi \cdot \nabla \eta = 0$ is enforced. Since derivatives of the coordinates have to be specified to satisfy orthogonality at the boundaries, specifying the location of the points overspecifies the problem with second-order partial differential equations as the grid generation system. Therefore, in order to generate a strictly orthogonal grid, the boundary points must be allowed to move on the boundary. In many cases this constitutes a major restriction on the generation of a useful grid. Therefore large values of λ'_o compared with values of λ'_s and λ'_w will only enhance the orthogonality of the grid. In general the grid is still nonorthogonal, and all terms in the governing transformed partial differential equations must be retained.

21. For a 2-D adaptive grid generator, partial differential equations

for the solution for the physical coordinates (x, y) are desired. These are obtained through the calculus of variations applied to the minimization of the sum of integrals in Equation 6. In general, if we wish to find functions $\phi_i(x, y)$ that are differentiable on (x, y) and satisfy fixed constraints on the boundary of the domain that minimize some integral functional

$$I = \int_D f \left(x, y, \phi_i, \frac{\partial \phi_i}{\partial x}, \frac{\partial \phi_i}{\partial y} \right) dx dy \quad (8)$$

the calculus of variations gives that $\phi_i(x, y)$ are the solutions of the Euler-Lagrange equations

$$\nabla \cdot \left[\frac{\partial f}{\partial (\nabla \phi_i)} \right] - \frac{\partial f}{\partial \phi_i} = 0 \quad (9)$$

22. The 2-D Euler-Lagrange equations for the minimization of the sum of integrals in Equation 6 are given by Brackbill and Saltzman (1982) as

$$\begin{aligned} b_1 x_{\xi\xi} + b_2 x_{\xi\eta} + b_3 x_{\eta\eta} + a_1 y_{\xi\xi} + a_2 y_{\xi\eta} + a_3 y_{\eta\eta} &= -J^2 \frac{\lambda_w}{2} w \frac{\partial w}{\partial x} \\ a_1 x_{\xi\xi} + a_2 x_{\xi\eta} + a_3 x_{\eta\eta} + c_1 y_{\xi\xi} + c_2 y_{\xi\eta} + c_3 y_{\eta\eta} &= -J^2 \frac{\lambda_w}{2} w \frac{\partial w}{\partial y} \end{aligned} \quad (10)$$

For completeness, the coefficients are reproduced from the cited paper and presented below:

$$a_i = \lambda_s a_{s_i} + \lambda_w w a_{w_i} + \lambda_o a_{o_i}$$

$$b_i = \lambda_s b_{s_i} + \lambda_w w b_{w_i} + \lambda_o b_{o_i} \quad i = 1, 2, 3$$

$$c_i = \lambda_s c_{s_i} + \lambda_w w c_{w_i} + \lambda_o c_{o_i}$$

$$a_{s1} = -A\alpha ; \quad b_{s1} = B\alpha ; \quad c_{s1} = C\alpha$$

$$a_{s2} = 2A\beta ; \quad b_{s2} = -2B\beta ; \quad c_{s2} = 12C\beta$$

$$a_{s3} = -AY ; \quad b_{s3} = BY ; \quad c_{s3} = CY$$

where

$$A = x_{\xi} y_{\xi} + x_{\eta} y_{\eta}, \quad B = y_{\xi}^2 + y_{\eta}^2, \quad C = x_{\xi}^2 + x_{\eta}^2$$

and

$$\alpha = \frac{x_{\eta}^2 + y_{\eta}^2}{J^3}, \quad \beta = \frac{x_{\xi} x_{\eta} + y_{\xi} y_{\eta}}{J^3}, \quad \gamma = \frac{x_{\xi}^2 + y_{\xi}^2}{J^3}$$

$$a_{w1} = -x_{\eta} y_{\eta}, \quad b_{w1} = y_{\eta}^2, \quad c_{w1} = x_{\eta}^2$$

$$a_{w2} = x_{\xi} y_{\eta} + x_{\eta} y_{\xi}, \quad b_{w2} = -2y_{\xi} y_{\eta}, \quad c_{w2} = -2x_{\xi} x_{\eta}$$

$$a_{w3} = -x_{\xi} y_{\xi}, \quad b_{w3} = y_{\xi}^2, \quad c_{w3} = x_{\xi}^2$$

$$a_{o1} = x_{\eta} y_{\eta}, \quad b_{o1} = x_{\eta}^2, \quad c_{o1} = y_{\eta}^2$$

$$a_{o2} = x_{\xi} y_{\eta} + x_{\eta} y_{\xi}, \quad b_{o2} = 2(2x_{\xi} x_{\eta} + y_{\xi} y_{\eta}), \quad c_{o2} = 2(x_{\xi} x_{\eta} + 2y_{\xi} y_{\eta})$$

$$a_{o3} = x_{\xi} y_{\xi}, \quad b_{o3} = x_{\xi}^2, \quad c_{o3} = y_{\xi}^2$$

Equation 10 constitutes the variational adaptive grid generator used in the present code.

Control Function Formulation

23. The elliptic generation system used in the WESCOR code is as follows:

$$\begin{aligned} \alpha x_{\xi\xi} - 2\beta x_{\xi\eta} + \gamma x_{\eta\eta} + \alpha P x_{\xi} + \gamma Q x_{\eta} &= 0 \\ \alpha y_{\xi\xi} - 2\beta y_{\xi\eta} + \gamma y_{\eta\eta} + \alpha P y_{\xi} + \gamma Q y_{\eta} &= 0 \end{aligned} \tag{11}$$

where now the coefficients are redefined as

$$\alpha = x_{\eta}^2 + y_{\eta}^2$$

$$\beta = x_\xi x_n + y_\xi y_n$$

$$\lambda = x_\xi^2 + y_\xi^2$$

Here P and Q are the control functions that serve to concentrate the grid lines.

24. In one dimension, with $y_\xi = x_n = 0$, these equations reduce to

$$x_{\xi\xi} + Px_\xi = 0$$

$$y_{nn} + Qy_n = 0$$

Now if the product of a weight function w and the grid spacing is equally distributed over the grid we have, in one dimension,

$$wx_\xi = \text{constant}$$

or

$$wx_{\xi\xi} + w_\xi x_\xi = 0$$

Then by analogy we make the connection

$$P = -\frac{x_{\xi\xi}}{x_\xi} = \frac{w_\xi}{w}$$

Generalizing we have

$$P = \frac{w_\xi}{w}, \quad Q = \frac{w_n}{w} \quad (12)$$

Equation 11, with the control functions evaluated from Equation 12, constitutes the adaptive generation system based on the original elliptic system of the WESCOR code.

PART III: DEPTH INTERPOLATION

25. A basic input to depth-averaged hydrodynamic models is the water depth associated with each computational cell. These depths, relative to some datum, are normally obtained from National Oceanic and Atmospheric Administration (NOAA) charts. An efficient grid generator that forces grid points to cluster in navigation channels through adaption to the water depth requires the interpolation of the input depth field determined from the NOAA charts. The number of input depth points and their distribution should be arbitrary. Various interpolation schemes that have been incorporated are discussed below.

Taylor Series Expansion About Nearest Depth Point

26. With (\bar{x}, \bar{y}) the nearest depth point to a grid point (x, y) , the depth $f(x, y)$ at the grid point is given by a Taylor series expansion about the depth point as follows:

$$\begin{aligned} f(x, y) = & f(\bar{x}, \bar{y}) + f_x(x - \bar{x}) + f_y(y - \bar{y}) + \frac{1}{2} f_{xx}(x - \bar{x})^2 \\ & + \frac{1}{2} f_{yy}(y - \bar{y})^2 + f_{xy}(x - \bar{x})(y - \bar{y}) + \dots \end{aligned} \quad (13)$$

where all derivatives are evaluated at the depth point.

27. These derivatives are determined by Taylor series expansions of the given depths at depth points neighboring the one in question about the latter (cf. Figure 1). Thus if the five nearest depth points to the depth point (\bar{x}, \bar{y}) are (x_i, y_i) $i = 1, 2, 3, 4, 5$, we then have

$$\begin{aligned} f_i = & f(\bar{x}, \bar{y}) + f_x(x_i - \bar{x}) + f_y(y_i - \bar{y}) \\ & + \frac{1}{2} f_{xx}(x_i - \bar{x})^2 + \frac{1}{2} f_{yy}(y_i - \bar{y})^2 \\ & + f_{xy}(x_i - \bar{x})(y_i - \bar{y}) \quad i = 1, 2, 3, 4, 5 \end{aligned} \quad (14)$$

Since the left sides here are known as values at depth points, this system constitutes five equations for the five derivatives at the depth point (\bar{x}, \bar{y}) . If fewer derivatives are included in the expansion about the depth point then

the number of equations in the system (14) is reduced accordingly. For example, for a linear expansion, only f_x and f_y are used in Equation 13, so only two neighboring depth points are used and the system (14) consists of two equations only. The code provides for the use of two (f_x, f_y) , three (f_x, f_y, f_{xy}) , four $(f_x, f_y, f_{xx}, f_{yy})$, and all five derivatives.

28. This interpolation is implemented by first sweeping all the depth points, at each of which the appropriate numbering of neighboring points is located and the required derivatives are evaluated by the solution of the system (14). Then the grid points are swept, determining the nearest depth point at each and determining the depth from Equation 13.

Interpolation Within Triangles or Quadrilaterals of Depth Points

29. If the depth at a grid point (x, y) is written as the linear function

$$f(x, y) = a + bx + cy \quad (15)$$

then the coefficients a , b , and c can be determined by evaluating Equation 15 at three depth points surrounding the grid point in question (cf. Figure 2). Thus we have the system

$$f_i = a + bx_i + cy_i \quad i = 1, 2, 3 \quad (16)$$

of three equations for the three coefficients.

30. Similarly, with the depth given by the product of linear functions in each coordinate we have

$$\begin{aligned} f(x, y) &= (a + bx)(c + dy) \\ &= ac + bcx + ady + bdxy \end{aligned}$$

Redefining the coefficients, this can be written as

$$f(x, y) = a + bx + cy + dxy \quad (17)$$

and now evaluation at four surrounding points gives the system

$$f_i = a + bx_i + cy_i + dx_iy_i \quad i = 1, 2, 3, 4 \quad (18)$$

31. Implementation proceeds by sweeping the grid points, at each of which the three or four nearest surrounding depth points are located and the coefficients are determined by solution of the system (16) or (18). Then the depth at the grid point is evaluated from Equation 15 or Equation 17.

Inverse-Power Interpolation Among Depth Points

32. Here the depth at a grid point (x, y) is written in terms of inverse powers of the distance to each point of a surrounding group of nearest depth points (cf. Figure 3) as follows:

$$f(x, y) = \frac{\sum_{i=1}^3 \frac{f(x_i, y_i)}{d_i^m}}{\sum_{i=1}^3 \frac{1}{d_i^m}} \quad (19)$$

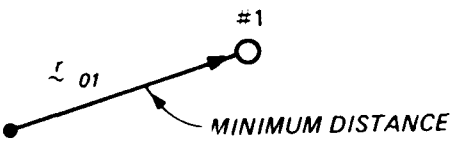
where $d_i = \sqrt{(x - x_i)^2 + (y - y_i)^2}$ is the distance from the grid point in question to the depth point (x_i, y_i) and m is a specified power, one or greater. The code provides for two, three, four, five, or all depth points to be used in Equation 19. The exponent m is an input quantity, higher values of this exponent giving sharper variations in depth.

Location of Neighboring Depth Points

33. The accuracy of the interpolation is enhanced if the group of depth points used generally surrounds the point in question. This requires a somewhat different selection procedure for each succeeding point chosen as described below. Each selected point is, of course, excluded from the selection procedure for the succeeding points.

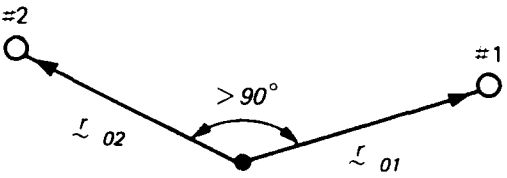
First point

34. The first depth point selected is simply the nearest one to the point in question: (The notation in all the following figures is that the vector ϵ_{ij} points from point i to point j , with the point about which the group is being formed designated as point 0.)



Second point

35. The second depth point selected is required to form an obtuse angle with the first point at the point in question. The closest point satisfying this requirement is the one chosen:

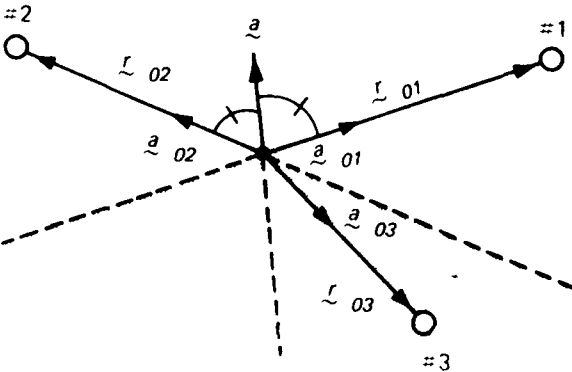


This is accomplished by selecting point 2 as the closest point having

$$r_{01} \cdot r_{02} \leq 0 \quad (20)$$

Third point

36. The third depth point chosen is the nearest one lying in the shaded zone in the figure below, i.e., between the backward extensions of the vectors to the first two points.



With the unit vectors to the selected points designated as \hat{a}_{01} , etc., the

unit vector \underline{a} along the bisector of the angle between the first two points is given by

$$\underline{a} = \frac{\underline{a}_{01} + \underline{a}_{02}}{|\underline{a}_{01} + \underline{a}_{02}|}$$

Then the third point will lie in the shaded region if

$$\underline{a}_{03} \cdot (-\underline{a}) \geq (-\underline{a}_{02}) \cdot (-\underline{a})$$

which, upon substitution for \underline{a} , becomes

$$1 + \underline{a}_{01} \cdot \underline{a}_{02} + \underline{a}_{02} \cdot \underline{a}_{03} + \underline{a}_{03} \cdot \underline{a}_{01} \leq 0$$

But

$$(\underline{a}_{01} + \underline{a}_{02} + \underline{a}_{03})^2 = 3 + 2(\underline{a}_{01} \cdot \underline{a}_{02} + \underline{a}_{02} \cdot \underline{a}_{03} + \underline{a}_{03} \cdot \underline{a}_{01})$$

so that the requirement becomes

$$1 + \left[\frac{1}{2}(\underline{a}_{01} + \underline{a}_{02} + \underline{a}_{03})^2 - \frac{3}{2} \right] \leq 0$$

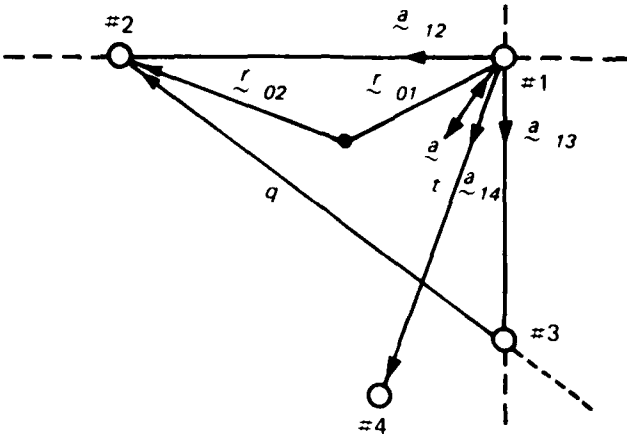
or finally simply that

$$|\underline{a}_{01} + \underline{a}_{02} + \underline{a}_{03}| \leq 1 \quad (21)$$

37. The nearest point satisfying this criterion is, of course, chosen. Selection of the third point in this manner assures that the point about which the group is formed will lie inside a triangle formed by the three depth points chosen.

Fourth point

38. The fourth point selected is required to lie outside the zones formed by extending the sides of the triangle of points already chosen:



In the diagram here, \underline{a} is the unit vector on the bisector of the angle between the vector from point 1 to points 2 and 3. Thus

$$\underline{a} = \frac{\underline{a}_{12} + \underline{a}_{13}}{|\underline{a}_{12} + \underline{a}_{13}|}$$

The fourth point will lie in the region between the extensions of the vectors \underline{a}_{12} and \underline{a}_{13} , as shown, if

$$\underline{a}_{14} \cdot \underline{a} \geq \underline{a}_{13} \cdot \underline{a}$$

Following a development analogous to that given above in connection with the third point, this becomes

$$|\underline{a}_{14} - \underline{a}_{12} - \underline{a}_{13}| \leq 1 \quad (22)$$

This, however, does not ensure that the fourth point is outside the triangle formed by the first three points. Therefore we require in addition that

$$|r_{14}| \geq t$$

Now

$$r_{01} + \underline{a}_{14}t + r_{02} + \underline{a}_{23}q$$

so that

$$\underline{a}_{14}t = \underline{a}_{23}q + \underline{r}_{12}$$

Crossing \underline{a}_{23} into both sides to eliminate q , we have

$$t = \frac{\underline{k} \cdot (\underline{a}_{23} \times \underline{r}_{12})}{\underline{k} \cdot (\underline{a}_{23} \times \underline{a}_{14})}$$

Point 4 then will lie outside the triangle if

$$|\underline{r}_{14}| > \frac{\underline{k} \cdot (\underline{a}_{23} \times \underline{r}_{12})}{\underline{k} \cdot (\underline{a}_{23} \times \underline{a}_{14})} \quad (23)$$

The inequalities (22) and (23) apply for a point outside the triangle and between the extensions of the sides with a vertex at point 1. Generalizing to the other two vertices, the fourth point is selected as the nearest point satisfying conditions (24) and (25) below for any of the three values of i , i.e., for any vertex of the triangle:

$$|\underline{a}_{14} - \underline{a}_{im} - \underline{a}_{in}| \leq 1 \quad (24)$$

$$|\underline{r}_{14}| > \frac{\underline{k} \cdot (\underline{a}_{mn} \times \underline{r}_{im})}{\underline{k} \cdot (\underline{a}_{mn} \times \underline{a}_{14})} \quad (25)$$

$$i = 1, 2, 3 \quad (i, m, n) \text{ cyclic}$$

Selection of the fourth point in this manner guarantees that the four points form a convex quadrilateral about the point in question.

Fifth point

39. Here again the nearest point is chosen, without regard to other considerations. This simple choice of the fifth point does not necessarily produce a convex polygon, but the extra complications involved in doing so was not considered justified in view of the lack of real incentive to use five points.

Additional groups

40. In some cases with fewer depth points it is possible that the interpolation is inaccurate because the particular group of points selected gives a false impression of very large gradients. Therefore provision is made for selecting more than one group of points and basing the interpolation on the group giving the smallest gradients. The code also automatically replaces points in any group leading to a zero determinant in the solution of the linear system for the derivatives or coefficients.

PART IV: GENERATION PROCEDURE

Iterative Solution

41. The numerical solution of Equation 10 or Equation 11 is accomplished in finite difference form by replacing all derivatives with second-order central difference expressions. The resulting difference equations are nonlinear since the coefficients of the second derivatives involve the first derivatives. This system of difference equations is solved by accelerated point Gauss-Seidel iteration. In both the first and second derivatives, all off-center values above, or to the right of, the point of evaluation are evaluated at the previous iteration, while those below, or to the left, are evaluated at the present iteration. With the central values in the second derivatives factored together, we then have a 2×2 system for x and y at the point in the case of Equation 10 and an uncoupled system with Equation 11. The field is swept repetitively until convergence to some prescribed tolerance.

Weight Function

42. The components of the gradient of the weight function are given by

$$w_x = \frac{1}{J} (w_{\xi} y_n - w_n y_{\xi}) \quad (26)$$

$$w_y = \frac{1}{J} (w_n x_{\xi} - w_{\xi} x_n)$$

and the values of the weight function at each point are continually updated during the iteration according to Equation 1. Since the weight function is not time-dependent on the physical field in the present application we have

$$\left(\frac{\partial w}{\partial t} \right)_{x,y} = 0$$

so that Equation 1 reduces to

$$\left(\frac{\partial w}{\partial t} \right)_{\xi,n} = \dot{x} w_x + \dot{y} w_y$$

Then using first-order forward difference expressions for the time derivatives and canceling the Δt we have

$$\Delta w = w_x \Delta x + w_y \Delta y \quad (27)$$

which could also have been obtained, of course, by direct application of the chain rule. Equation 27 then serves to determine the change in w at each point in terms of the change in x and y at each iteration.

43. The code first generates a grid from the original WESCOR system without adaption. Depth values are then interpolated onto this initial grid from the set of depth points. The depth points may be input in any order and without any pattern. The code automatically adds the points on the outer boundary to the input set of depth points, with a depth of zero for the former, and eliminates duplicated points. It is this augmented set that is used in the interpolation. These zero depths on the outer boundary can be overridden by including the outer points that are to have nonzero depth in the input set of depth points. Several forms of interpolation are provided as discussed in PART III. After the interpolation the depths can be smoothed on the initial grid points.

44. The smoothed interpolated values of the depth on the initial grid then are used as the weight function in the generation system, the values of the depth being continually updated at each point from Equation 13 as the grid moves without further interpolation.

Input

45. The depth-adaptive code, called WESCORA, has the same structure as the earlier WESCOR code capable of generating 2-D grids on arbitrary regions with interior obstacles. The input is the same as that described for the WESCOR code by Thompson (1983), with a few additions described below. Complete input instructions for WESCORA are given in Appendix A.

46. The total number of depth points to be read in for grid adaption is input as NDEP, and a flag NDOP controls the printing of the depth points. (If NDEP=0 the code runs the nonadaptive system only.) The flag NDEPF causes the depth points to be read from file 12 instead of from the input. The type of interpolation is specified by NINP as follows:

NINP = 0	:	inverse-power interpolation using all points
-2	:	inverse-power interpolation using 2 points
-3	:	inverse-power interpolation using 3 points
-4	:	inverse-power interpolation using 4 points
-5	:	inverse-power interpolation using 5 points
2	:	Taylor series interpolation using 2 points
3	:	Taylor series interpolation using 3 points
4	:	Taylor series interpolation using 4 points
5	:	Taylor series interpolation using 5 points
13	:	Bilinear interpolation using 3 points
14	:	Bilinear interpolation using 4 points

If adjusted depths are used for the adaption, then an additional depth file containing actual depths is input to provide real depths at the center of each computational cell. The flag LDEPF causes the second set of depth points to be read from file 16 instead of from the input, with LDEP points contained in the file. The interpolation of the actual depth field onto the final adaptive grid can be a different type from that employed in the grid generation. The types available are the same as those described above. The use of an adjusted depth field is discussed in more detail in PART V.

47. The parameter NCOM specifies the number of groups of points to be considered in the interpolation (the default is one group). The parameter NTES suppresses the requirement that the points selected form a convex polygon about the point in question, and the parameter NSMO suppresses the smoothing of the depths after interpolation onto the grid points.

48. The three parameters controlling the relative emphasis on concentration, smoothness, and orthogonality are input as WFACI, SFAC, and OFACI, respectively, the nominal ranges being 0-1. (A negative value of WFACI will cause the control function adaption, rather than the variational adaption, to be used, with the magnitude in the nominal range. In this case the other two parameters are irrelevant.)

49. The depth points used in the adaption are read in either from the input or from file 12, immediately after the boundary points are read, with the Cartesian coordinates of the point in columns 0-10 and 11-20, and the depths in columns 21-30. The depth points may be in any order, and duplications will be automatically eliminated by the code. If a second set of depth

points is input, they are read in either from the input or from file 16. The format is the same as noted above.

50. An additional feature has also been added allowing the use of Neumann boundary conditions to produce orthogonality on straight boundaries if desired. This feature is activated by NEUBOD for slab sides and by NEUOUT for the outer boundary.

PART V: CHESAPEAKE BAY APPLICATION

51. For demonstration purposes, the adaptive grid generation code WESCORa has been applied to Chesapeake Bay (Figure 4).

Chesapeake Bay

52. Chesapeake Bay, located on the east coast of the United States, is one of the largest estuaries in the world. The main bay extends approximately 190 miles north from the ocean entrance in the Commonwealth of Virginia, between Cape Henry and Cape Charles, to the Susquehanna River in the State of Maryland. The average depth of the bay is about 28 ft, although a natural channel with depths greater than 50 ft traverses the bay for more than 60 percent of its length. The maximum depth of 175 ft is located in the upper bay near Bloody Point, Kent Island, Maryland.

53. Like many coastal plain estuaries, the bay is irregular in shape varying in width from 4 miles, between Annapolis and Kent Island, to 30 miles, in the middle bay off the Potomac River. More than 64,000 square miles of drainage area empty into the bay through more than 50 different tributary systems. Five major western shore rivers (Susquehanna, Potomac, James, York, and Rappahannock) provide approximately 90 percent of the annual freshwater discharge.

Selection of Boundary Points

54. A basic input to the grid generation code is the specification of the (x,y) coordinates of the boundary points (Figure 5). The degree of resolution of boundary features will, of course, depend upon the number of ξ and η lines selected in the transformed rectangular plane as well as the location of the boundary points. The actual boundary points selected for use in WESCORa are listed in Appendix B. Figure 5 is presented only for demonstration purposes. The rectangular (ξ,η) plane corresponding to the actual boundary points listed in Appendix B is shown in Figure 6.

Grid Generation Using Actual Depths

55. Initially, depth points were randomly selected, with approximately 800 points specified to cover the navigation channel as well as the nonchannel areas. Depths ranging from 0 on the boundary to a maximum of 156 ft were input. All of the interpolation schemes previously discussed were tried with little success in forcing coordinate lines to closely follow the navigation channel. The grid presented in Figure 7, which resulted from a 3-point inverse power interpolation with an exponent of 4 (Equation 19), does show some adaption to the channel. However, the depth field interpolated on the initial grid presented in Figure 8 evidently did not contain sufficient gradients to force adequate adaption to the natural channel. The concentration evident in this initial grid is caused by the boundary point distribution through the control functions in the original WESCOR formulation as mentioned in paragraph 6. Another example is the grid shown in Figure 9, which was computed using 2-point inverse power interpolation with the exponent set to be 10. The grid seems to be trying to adapt to two channels. The reason is not apparent.

Grid Generation Using Hypothetical Depths

56. The next effort involved using an adjusted depth field in which the natural channel was assumed to be 100 ft deep, with zero depths specified out of the channel. In addition, as illustrated in Figure 10, the depths were read in as points of cross sections that were constructed approximately perpendicular to the center line of the channel. A total of approximately 100 depth points, with a value of either 0 or 100, were input.

57. With the hypothetical depth field, attraction of grid points to the navigation channel was achieved for most of the interpolation schemes. The 4-point bilinear with smoothing and the 3-point bilinear with no smoothing schemes resulted in unstable computations. However, the 3-point bilinear scheme with smoothing was stable and the resulting coordinate system, presented in Figure 11, contains good clustering of grid points in the channel. Figures 12 and 13 show grids generated using the 2-point inverse power interpolation with exponents of 4 and 10, respectively. Little impact as a result of the change in the exponent is observed. The grid presented in Figure 14 resulted from using 4-point inverse power interpolation with an exponent of 4,

while that in Figure 15 used a Taylor series interpolation with 2 points. The latter is perhaps the most physically appealing of all the grids generated.

Influence of Weighting Factors

58. All of the grids presented up to now were generated with a weighting factor of 1.0 for each of the three contributing integrals in Equation 10. To demonstrate the relative effect of each factor, Figures 16 and 17 are presented. In Figure 16, the concentration weight factor has been set to 0.0, with the smoothness and orthogonality factors retaining a value of 1.0. As expected, no attraction to the navigation channel occurs and a relatively smooth grid is generated. This occurs even though the initial grid, shown in Figure 8, had concentration based upon boundary point distribution. The variational formulation with only smoothness and orthogonality smooth out the initial concentration. In Figure 17, both the concentration factor and the orthogonality factor are set to 0.0, while keeping the smoothness factor at 1.0. This is the grid that would be computed by the WESCOR code with zero values for the control functions in Equation 11. An interesting observation is that the grid generated with no enhancement of orthogonality, i.e., Figure 17, would probably be more appropriate for flow computations than the one in which the orthogonality condition is enforced, i.e., Figure 16, because orthogonality is achieved at the expense of smoothness.

Practical Aspects

59. Obviously, not only the numerical grid, in which grid lines follow navigation channels, but also the water depths associated with each computational cell are desired as output from the grid generator. The numerical hydrodynamic-transport model to be subsequently employed would then use this output in the computation of flow and constituent fields. However, use of the actual depth field, input as a random distribution, did not result in sufficient depth gradients to force grid lines to adequately follow the natural navigation channel in Chesapeake Bay. As a result, a hypothetical depth field was created, with large depths in the channel and zero values elsewhere. In this case, the final depth associated with each computational cell is meaningless. It should be realized that as far as grid generation is concerned the

use of either real or adjusted depths is immaterial, although real depths are required on the final grid upon which flow computations are to be made. The solution is to use the adjusted depth field to compute the grid and then to interpolate from the actual depth field for the water depth to be associated with each cell of the final grid.

60. Based upon the Chesapeake Bay grid generation, it appears that the Taylor series interpolation with 2 points yields perhaps the "best-looking" adaptive grid. Evidently the gradients in the hypothetical field are better maintained after interpolation onto the initial grid, although the actual values are in error. Table 1 presents the depth limits resulting from different interpolation schemes, along with the limits of the interpolated depth field after smoothing. Based upon the results shown in Table 1, it would appear that interpolation of the actual depth field onto the final adaptive grid should perhaps be based upon the inverse power interpolation with no smoothing.

PART VI: SUMMARY AND CONCLUSIONS

Summary

61. As a result of the need for generating boundary-fitted numerical grids for use with finite difference models in coastal and estuarine areas, a numerical grid generation code called WESCORA has been developed as an extension of an earlier code, called WESCOR. Grid generation is based upon adaptive grid techniques that have been developed for dynamic grid adaption. However, for the purpose of computing free-surface hydrodynamics and transport in coastal and estuarine areas these techniques have been employed here only for the generation of the initial grid and no time-dependence is considered.

62. Two adaptive mechanisms are contained in WESCORA; namely, adaption based upon a variational formulation and adaption based upon a control function formulation. In both cases, adaption to water depths is used to force grid lines to follow navigation channels. Preliminary testing of the two approaches has shown that the variational formulation is apparently the more reliable.

63. In the variational approach, a functional that consists of the sum of three integrals involving the physical coordinates is minimized over the grid. The first of the integrals controls grid point concentration while the other two control grid smoothness and skewness of the grid lines. By weighing the importance of the three integrals, either grid point concentration, smoothness, or orthogonality can be emphasized.

Conclusions

64. Preliminary testing of WESCORA on Chesapeake Bay has resulted in the general conclusion that numerical grids can be generated such that grid points cluster in navigation channels. However, unless there are large differences between the channel and nonchannel depths, a fictional depth field may be required to achieve adequate adaption. In this case, the actual depth field should be interpolated onto the final adaptive grid to provide relatively accurate water depths to be associated with each computational cell of the grid. Particular conclusions concerning usage of the code are offered below.

- a. The inverse power interpolation is bounded by the extreme values of the depth values and is the smoothest interpolation. It may give, however, a depth distribution that is smoother than intended. A value of 2 to 4 for the exponent involved here is probably appropriate.
- b. There is probably no real reliable advantage to using large numbers of points in the interpolation, three points being most reasonable.
- c. The features provided requiring a convex polygon of depth points in the interpolation and smoothing after the interpolation should be used.
- d. Multiple groups of interpolation points should be used with the Taylor series and bilinear interpolations, four groups being reasonable.
- e. For grid generation, the bilinear interpolation with three points or the Taylor series interpolation with two points, should be good choices in most cases. The inverse power interpolation with no smoothing should provide relatively accurate depths on the final grid.
- f. Neumann boundary conditions (orthogonality at the boundary) should be used on boundary segments on which the depth varies. This feature requires that the boundary segment in question be straight.
- g. The variational adaptive mechanism is the more reliable. The values of the smoothing and orthogonality parameters should be kept equal and not more than an order of magnitude smaller than the concentration parameter in most cases.
- h. If the randomly distributed depth field does not yield depth gradients sufficient to cause good adaption to navigation channels, a hypothetical field such as the one used in the Chesapeake Bay example should be input. In general, cross sections should be aligned perpendicular to the channel.

REFERENCES

- Brackbill, J. V., and Saltzman, J. S. 1982. "Adaptive Zoning for Singular Problems in Two Dimensions," Journal of Computational Physics, Vol 46.
- Johnson, B. H. 1980. "VAHM - A Vertically Averaged Hydrodynamic Model Using Boundary-Fitted Coordinates," Miscellaneous Paper HL-80-3, US Army Engineer Waterways Experiment Station, Vicksburg, Miss.
- Johnson, B. H., Thompson, J. F., and Baker, A. J. 1984. "A Discussion of Adaptive Grids and Their Applicability in Numerical Hydrodynamic Modeling," Miscellaneous Paper HL-84-4, US Army Engineer Waterways Experiment Station, Vicksburg, Miss.
- Sheng, Y. P., and Hirsh, J. E. 1984. "Numerical Solution of Shallow Water Equations in Boundary-Fitted Grid," prepared for CERC, US Army Engineer Waterways Experiment Station, Vicksburg, Miss.
- Thompson, J. F. 1983. "A Boundary-Fitted Coordinate Code for General Two-Dimensional Regions with Obstacles and Boundary Intrusions," Technical Report E-83-8, US Army Engineer Waterways Experiment Station, Vicksburg, Miss.
- . 1985. "A Survey of Dynamically Adaptive Grids in the Numerical Solution of Partial Differential Equations," Applied Numerical Mathematics, Vol 1.
- Thompson, J. F., Thames, F. C., and Mastin, C. W. 1977. "TOMCAT - A Code for Numerical Generation Systems on Fields Containing Any Number of Arbitrary Two-Dimensional Bodies," Journal of Computational Physics, Vol 24.
- Thompson, J. F., Warsi, Z. V. A., and Mastin, C. W. 1985. Numerical Grid Generation, North Holland, Elsevier Science Publishing Co., New York.

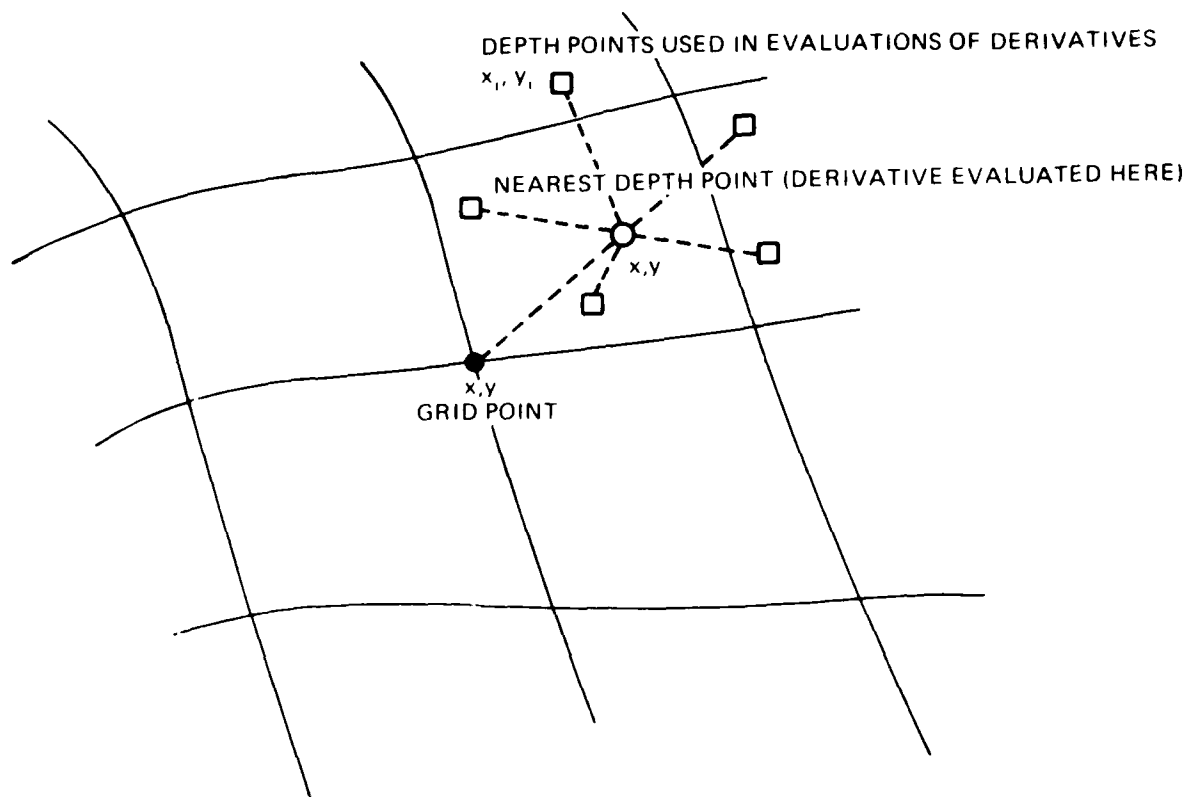


Figure 1. Taylor series expansion about nearest depth point

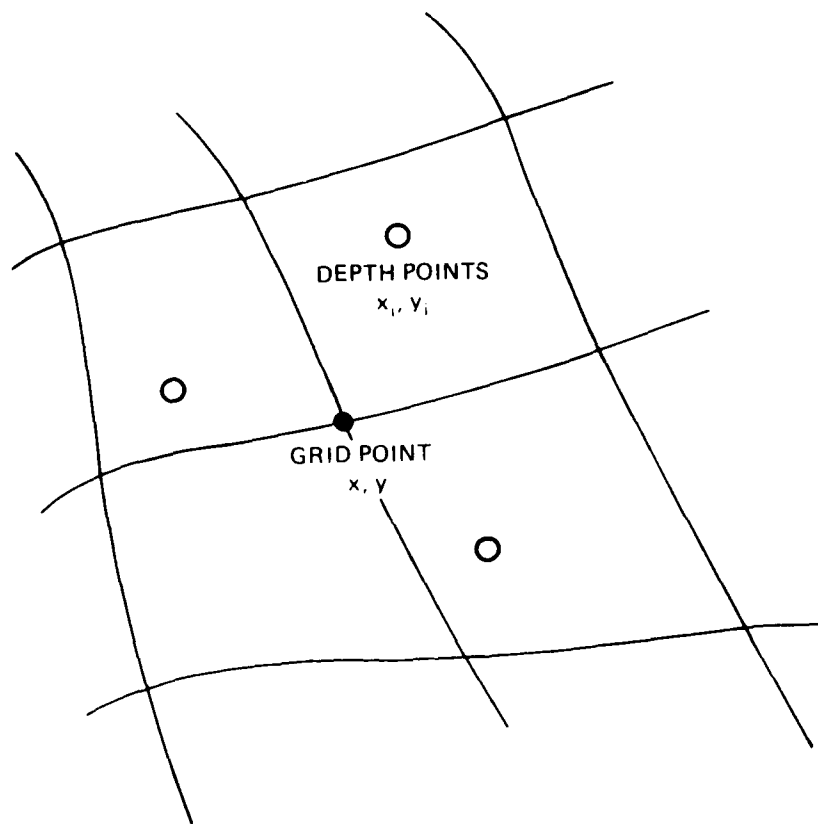


Figure 2. Bilinear interpolation within triangle of depth points

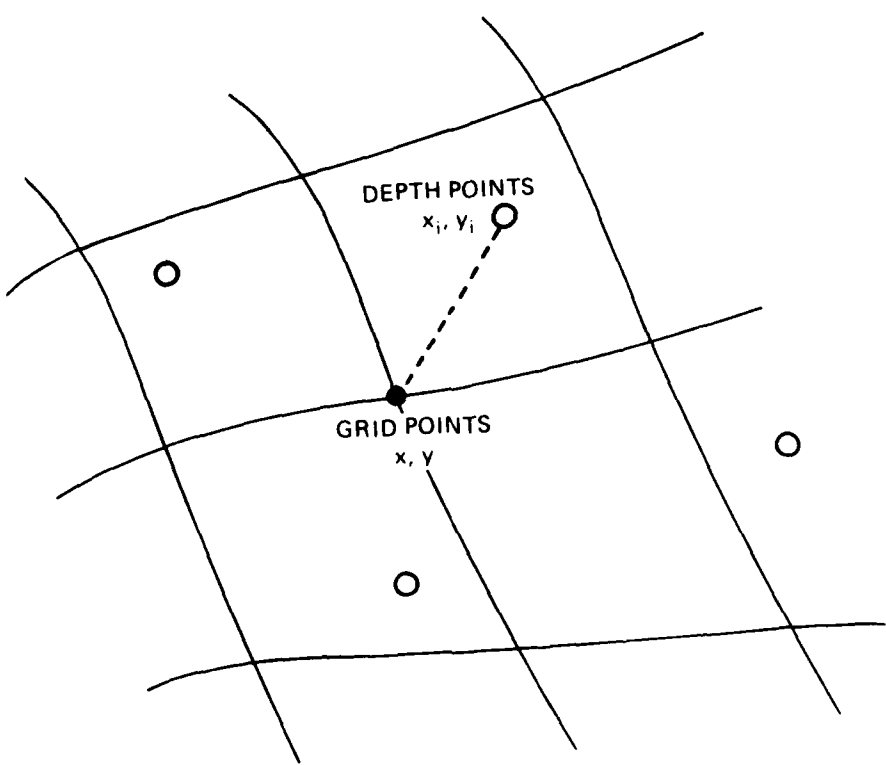


Figure 3. Inverse power interpolation
among depth points

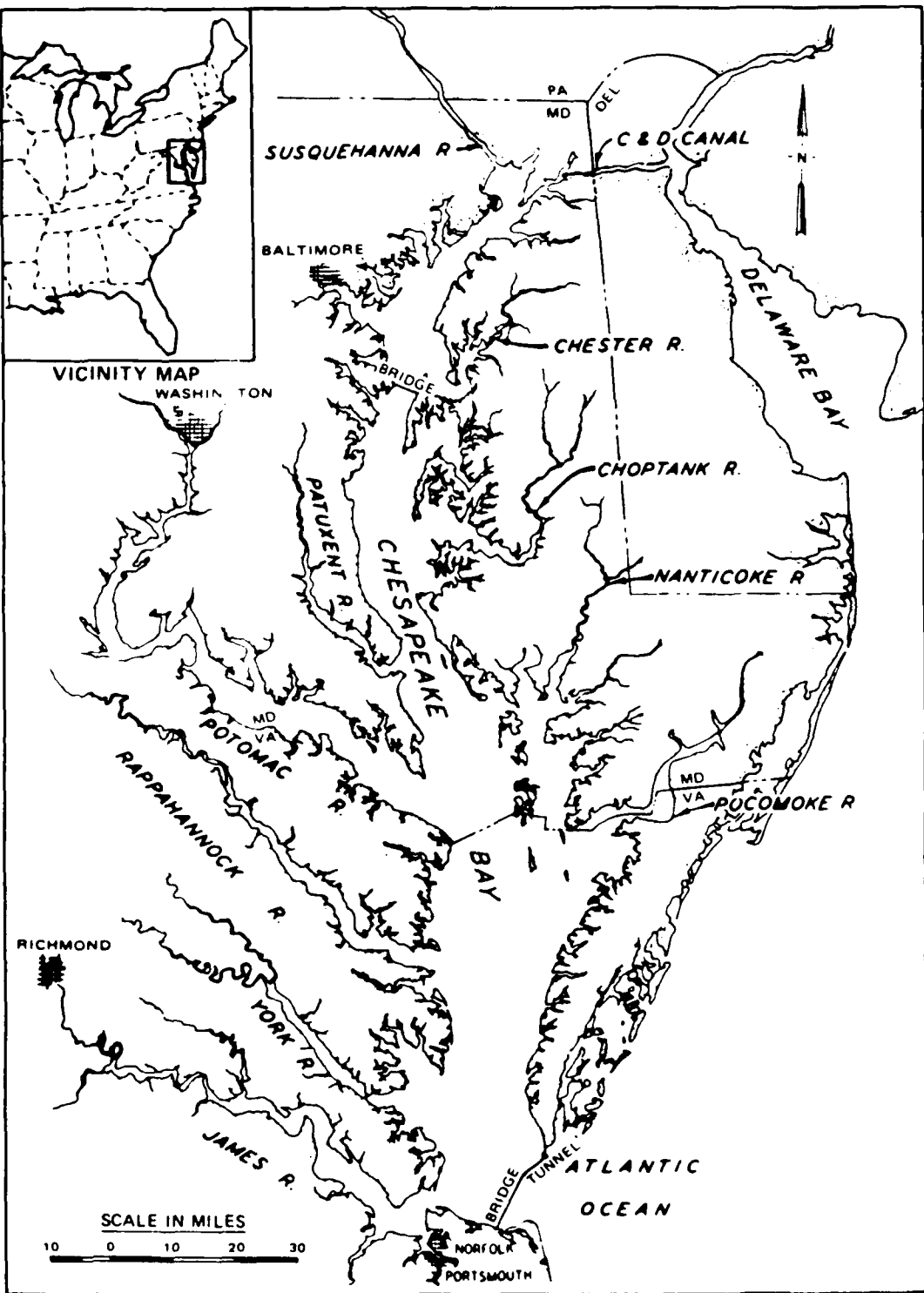


Figure 4. Location map

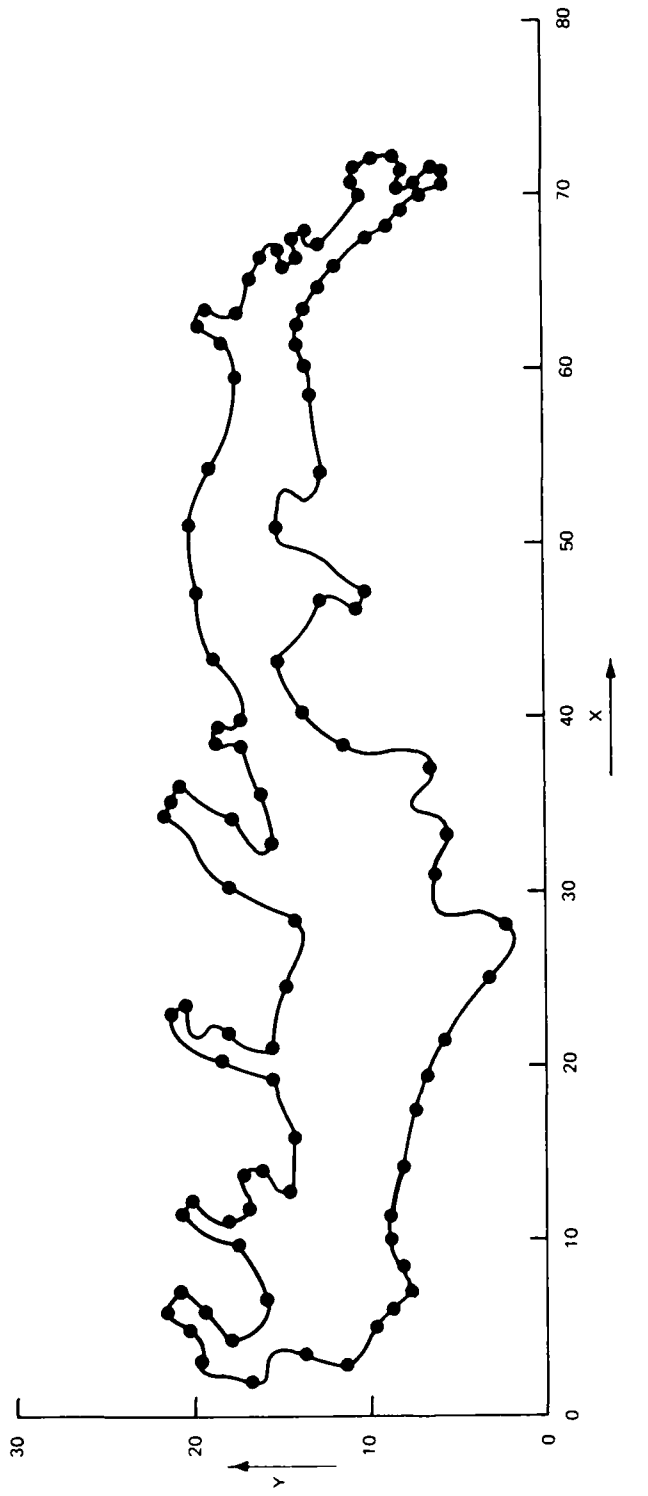


Figure 5. Boundary point data

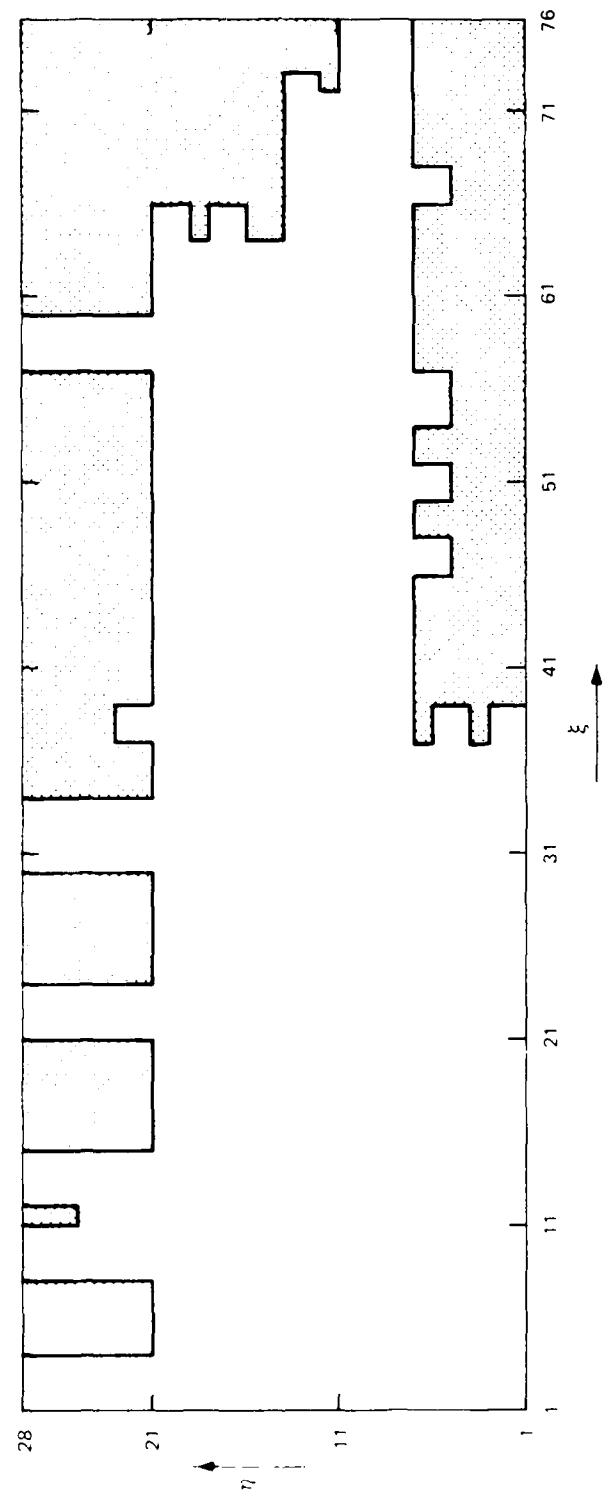


Figure 6. Transformed rectangular plane

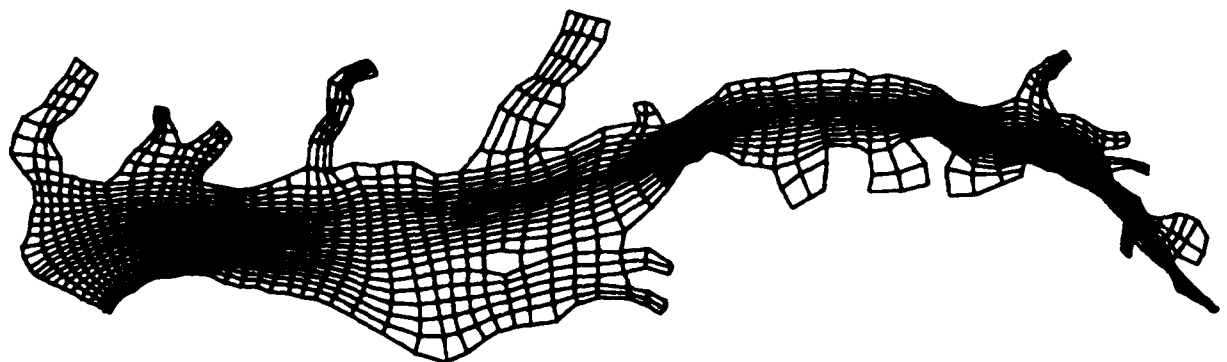


Figure 7. Depth-adaptive grid using inverse power interpolation
with three points and an exponent of 4

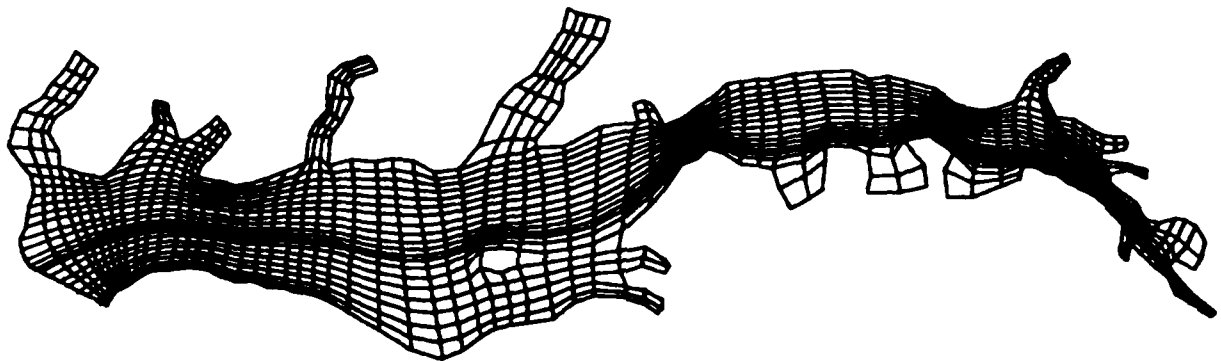


Figure 8. Initial grid

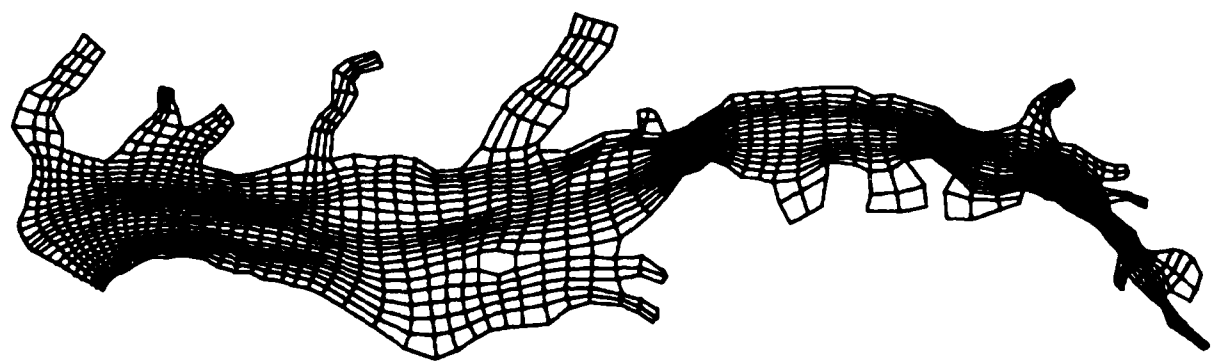


Figure 9. Depth-adaptive grid using inverse power interpolation
with two points and an exponent of 10

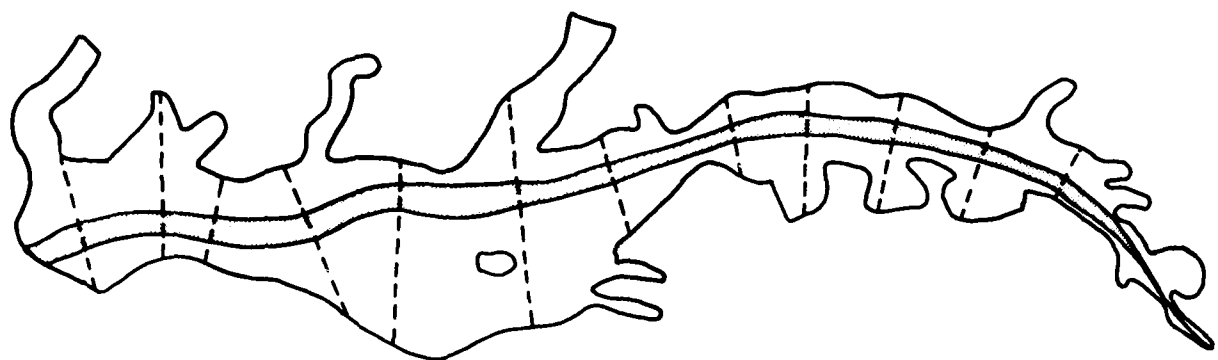


Figure 10. Demonstration of depths input from cross sections

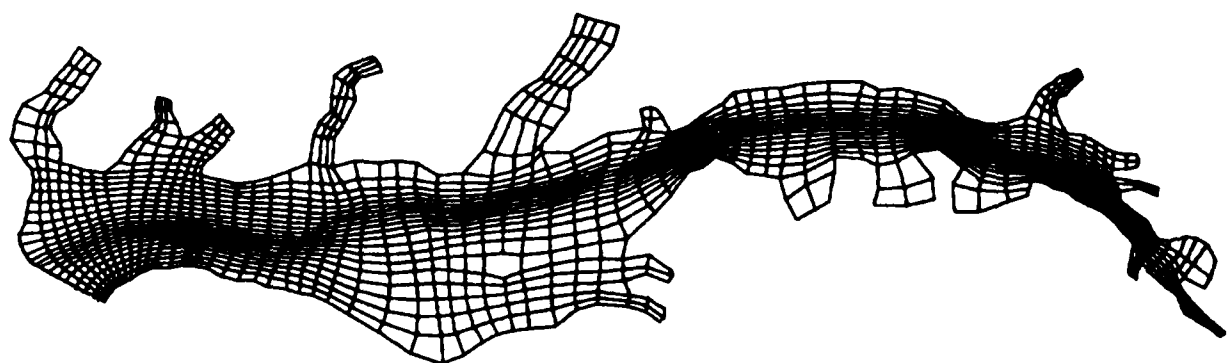


Figure 11. Depth-adaptive grid using bilinear interpolation
with three points

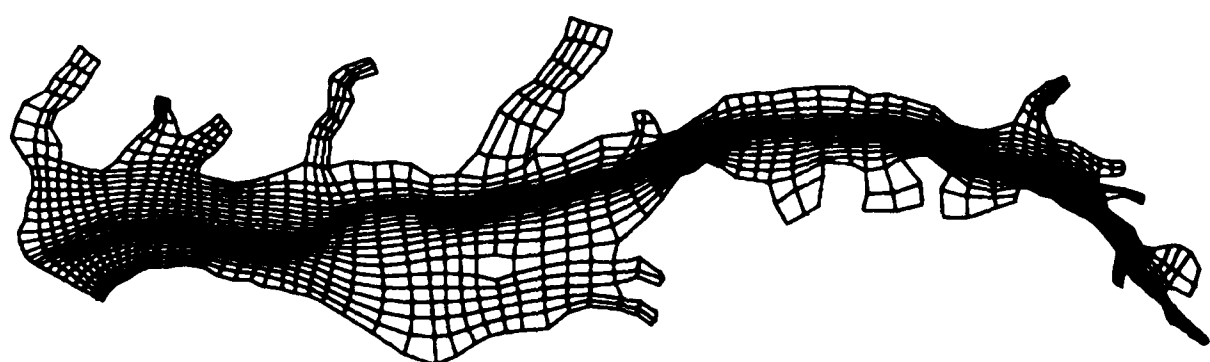


Figure 12. Depth-adaptive grid using inverse power interpolation
with two points and an exponent of 4

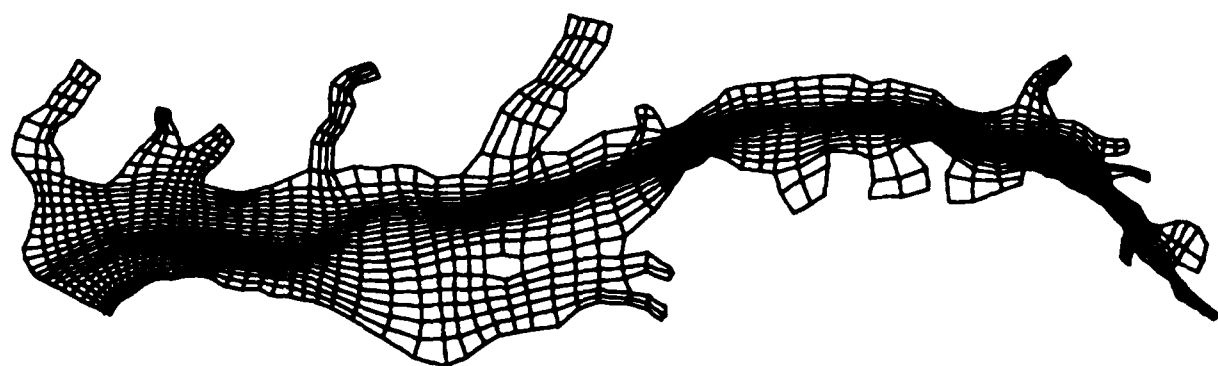


Figure 13. Depth-adaptive grid using inverse power interpolation
with two points and an exponent of 10

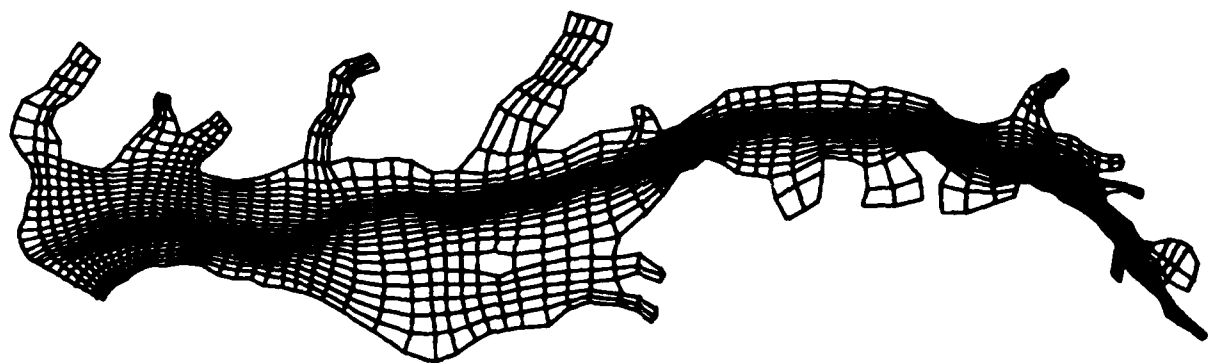


Figure 14. Depth-adaptive grid using inverse power interpolation
with four points and an exponent of 2

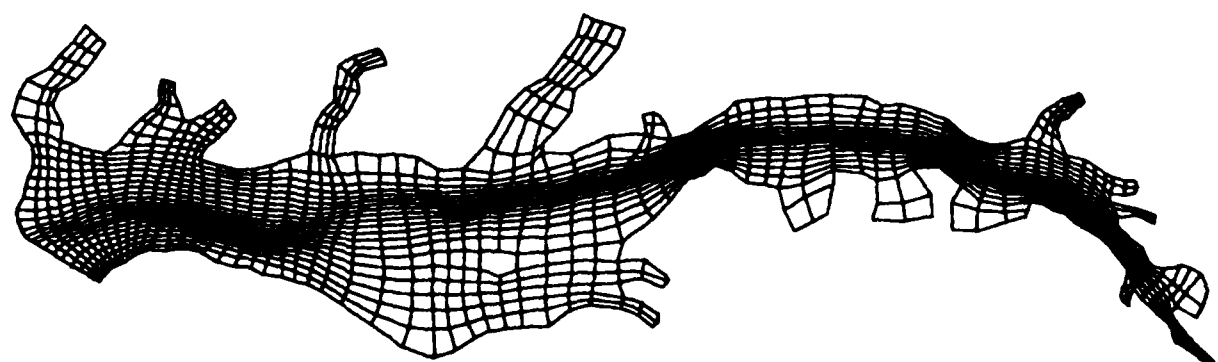


Figure 15. Depth-adaptive grid using Taylor series interpolation
with two points

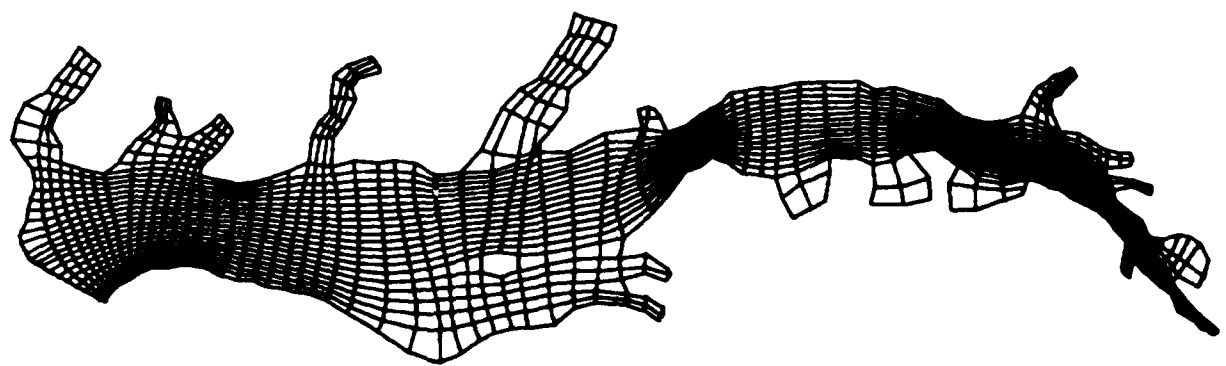


Figure 16. Depth-adaptive grid with concentration factor = 0.0
and orthogonality and smoothness factors = 1.0

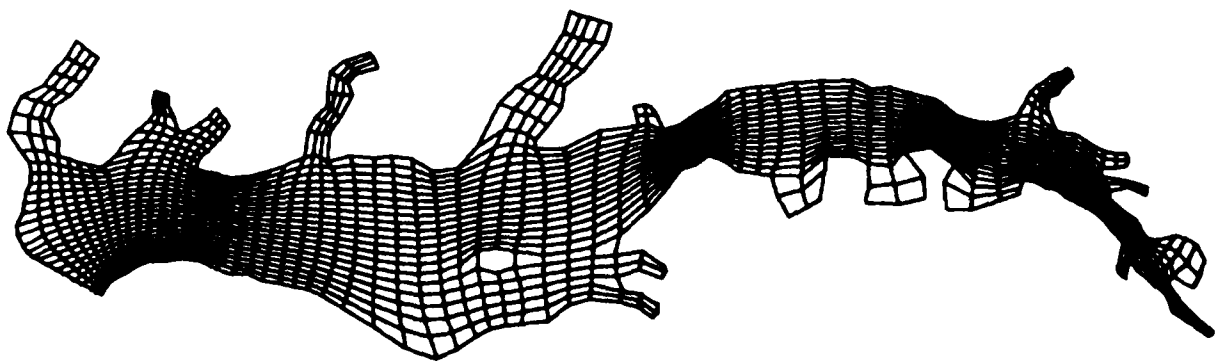


Figure 17. Depth-adaptive grid with concentration and
orthogonality factors = 0.0 and smoothness factor = 1.0

Table 1
Interpolated Depth Limits

<u>Interpolation Scheme</u>	<u>Actual Limits</u>	<u>Interpolated Limits</u>	<u>Smoothed Limits</u>
Bilinear with 3 points	0-156	0-120	0- 86
Bilinear with 3 points	0-100	0-100	0- 98
Inverse power with 4 points, exponent = 4	0-156	0-137	0-100
Inverse power with 4 points, exponent = 2	0-100	0-100	0- 95
Inverse power with 3 points, exponent = 4	0-156	0-137	0-100
Inverse power with 3 points, exponent = 4	0-100	0-100	0-100
Taylor series with 2 points	0-156	0-139	1- 96
Taylor series with 2 points	0-100	0-449	1-296
Taylor series with 3 points	0-156	0-204	1-126

APPENDIX A: INPUT INSTRUCTIONS

```

XXXXXXXXXXXXXXXXXXXXXXXXXXXXXXXXXXXXXXXXXXXXXX
C
CXXXXXXXXXXXXXXXXXXXXXXXXXXXXXX W E S C O R A XXXXXXXXXXXXXXXXXXXXXXXXXXXXXXXXX
C
CXXXXXXXXXXXXXXXXXXXXXXXXXXXXXX
C
C 2-D BOUNDARY-FITTED COORDINATE SYSTEM CODE ( DEPTH-ADAPTIVE )
C
C MISSISSIPPI STATE UNIVERSITY . 1982      REVISED 1985
C
C U.S. ARMY ENGINEER WATERWAYS EXPERIMENT STATION
C VICKSBURG, MISSISSIPPI
C
CXXXXXXXXXXXXXXXXXXXXXXXXXXXXXX
C
C XXXXXXXXXX SLIT-SLAB CONFIGURATION XXXXX
C
C XXXX ATTRACTION TO COORDINATE LINES/POINTS AND TO SPACE LINES/POINTS.
C XXXX CONTROL FUNCTIONS ALSO INTERPOLATED FROM BOUNDARY POINT DISTRIBUTION
C
C XXXX ADAPTIVE ON DEPTH DISTRIBUTION.
C
C XXXX CAN BE ORTHOGONAL ON STRAIGHT BOUNDARY SEGMENTS.
C
C XXXXXXXXXX INPUT INSTRUCTIONS :
C
C XXX CARDS(2) : LABEL - FORMAT(10A8)
C
C           LABEL - TWO 80 CHARACTER CARDS. (BLANK CARDS IF NO LABEL)
C
C XXX CARD : IMAX,JMAX,NBDY,ITER,ISLIT,IBNDRY,IDISK,IWIR,IUINTL,
C           IUFIM,MREM,MEUINT - FORMAT(12I5)
C
C           IMAX - NUMBER OF XI POINTS.
C
C           JMAX - NUMBER OF ETA POINTS.
C
C           NBDY - TOTAL NUMBER OF SLAB SIDES AND SLITS IN THE FIELD.
C
C           ITER - MAXIMUM NUMBER OF ITERATIONS ALLOWED.
C
C           ISLIT - -1 SLAB SIDES OR SLITS READ FROM CARDS.
C                   X,Y - FORMAT(2F10.0), ONE POINT PER CARD.
C                   -2 SLAB SIDES OR SLITS READ FROM FILE 10.
C                   X,Y - FORMAT(2F10.0), ONE POINT PER CARD.
C
C           (NOTE: HORIZONTAL SLITS ARE READ CLOCKWISE FROM RIGHT END.)
C           ( VERTICAL SLITS ARE COUNTER-CLOCKWISE FROM TOP. )
C           ( SLAB SIDES MAY BE READ IN EITHER DIRECTION. )
C
C           IBNDRY - -0 OUTER BOUNDARY CALCULATED INTERNALLY AS CIRCLE.
C                   -1 OUTER BOUNDARY READ FROM CARDS.
C                   X,Y - FORMAT(2F10.0), ONE POINT PER CARD.
C                   -2 OUTER BOUNDARY READ FROM FILE 10.
C                   X,Y - FORMAT(2F10.0), ONE POINT PER CARD.
C                   --1 OUTER BOUNDARY READ IN SEGMENTS AS SLAB SIDES.
C
C           (NOTE: FOR IBNDRY = 1 OR 2, OUTER BOUNDARY IS READ CLOCKWISE
C           ( FROM POINT (INFXI,INFETA).

```

'OUTER BOUNDARY' MEANS ENTIRE BOUNDARY OF TRANSFORMED REGION IF NREM=0. IF NREM IS NOT ZERO, THEN OUTER BOUNDARY IS THE TOP OF THE TRANSFORMED REGION AND INNER BOUNDARY IS THE BOTTOM.

IDISK - •0 DON'T READ OR WRITE SYSTEM FROM OR ON FILE.
 •1 WRITE SYSTEM ON FILES 10 & 11. DON'T READ SYSTEM FR
 •2 WRITE SYSTEM ON FILES 10 & 11 . READ SYSTEM FROM FI
 •3 READ SYSTEM FROM FILE 10 FOR RESTART. DON'T WRITE S

(NOTE: FILE 10 IS RESTART FILE FOR CONTINUATION OF ITERATION.)
 (FILE 11 IS STORAGE FILE FOR FINAL SYSTEM.)

IUIR - •0 DON'T PRINT EACH ITERATION ERROR.
 •1 PRINT EACH ITERATION ERROR.

IUIMTL - •0 DON'T PRINT INITIAL GUESS.
 •1 PRINT INITIAL GUESS.

IUFIM - ZERO SUPPRESSES PRINT OF FINAL VALUES.

NREM - NON-ZERO USES RE-ENTRANT BOUNDARY ON LEFT & RIGHT SIDE OF TRANSFORMED REGION, WITH OUTER BOUNDARY ON TOP AND INNER BOUNDARY ON BOTTOM.

INNER BOUNDARY IS READ AS FOLLOWS BEFORE READING OUTER
 -1 INNER BOUNDARY READ FROM CARDS.
 X,Y - FORMAT(2F10.0) , ONE POINT PER CARD.
 -2 INNER BOUNDARY READ FROM FILE 10.
 X,Y - FORMAT(2F10.0) , ONE POINT PER CARD.

(NOTE: SLITS AND/OR SLABS MAY ALSO BE PRESENT.)

NEUINT - 1 SUPPRESSES NEUMANN BOUNDARY CONDITIONS FOR INITIAL GRID.

NBDY) LB1,LB2,LB3,LTYPE,NEUBOD - FORMAT(5I5)

LB1,LB2 - FIRST AND LAST INDICES OF SLAB SIDE OR SLIT ENDS.
 (LB2 MAY BE LESS THAN LB1 FOR SLAB SIDE. INPUT IS FRO

LB3 - INDEX OF LINE ON WHICH SLAB SIDE OR SLIT IS LOCATED.

LTYPE - SLAB SIDE OR SLIT TYPE (1 FOR HORIZONTAL, 2 FOR VERTICA
 (NEGATIVE INDICATES SLAB SIDE, RATHER THAN SLIT.)
 (SUBTRACT 10 FOR OUTER BOUNDARY SEGMENT.)
 (I.E., -11 IS HORIZONTAL OUTER BOUNDARY SEGMENT,)
 (-12 IS VERTICAL OUTER BOUNDARY SEGMENT.)

NEUBOD - 1 MEANS NEUMANN BOUNDARY CONDITION.
 0 MEANS DIRICHLET CONDITION.

NEUOUT(4) - FORMAT(4I5)

NEUOUT - 1 MEANS NEUMANN BOUNDARY CONDITIONS ON OUTER BOUNDARY.
 (OUTER BOUNDARY MADE OF SLAB SIDES IS CONTROLLED BY NEUBOD INSTEAD OF NEUOUT.)
 0 MEANS DIRICHLET CONDITIONS.

```

C   : (1) : LEFT
C   : (2) : RIGHT
C   : (3) : BOTTOM
C   : (4) : TOP
C
C88 CARD : NDEP,NDOUT,NDOP,NDEPF,NIMP,NCOM,NTES,NSMO - FORMAT(8I5)
C
C   NDEP - NUMBER OF DEPTH POINTS.
C   ( ZERO FOR NON-ADAPTIVE SYSTEM )
C
C   NDOUT - NON-ZERO ADDS OUTER BOUNDARY POINTS TO DEPTH POINT
C   LIST, WITH ZERO DEPTH.
C   ( THIS SHOULD BE USED UNLESS THE INPUT DEPTH POINTS
C   EXTEND TO OR BEYOND THE OUTER BOUNDARY. INPUT DEPTH
C   POINTS THAT ARE COINCIDENT WITH OUTER BOUNDARY POINTS
C   WILL RETAIN THE INPUT DEPTH EVEN WHEN THIS FEATURE
C   IS USED. )
C
C   NDOP - 1 PRINTS DEPTH POINTS.
C
C   NDEPF - NON-ZERO READS DEPTH POINTS FROM FILE 12.
C
C   NIMP - INTERPOLATION TYPE : 0 > HARMONIC - ALL
C   13 > BILINEAR - 3 POINTS
C   14 > BILINEAR - 4 POINTS
C   2 > 2-POINT TAYLOR SERIES
C   3 > 3-POINT TAYLOR SERIES
C   4 > 4-POINT TAYLOR SERIES
C   5 > 5-POINT TAYLOR SERIES
C   -2 > HARMONIC - 2 POINTS
C   -3 > HARMONIC - 3 POINTS
C   -4 > HARMONIC - 4 POINTS
C   -5 > HARMONIC - 5 POINTS
C
C   ( BEST ARE 13 , 2 , 3 , -2 , -3 )
C
C   NCOM - NUMBER OF INTERPOLATION POINT SETS FOR TAYLOR. ( 4 )
C   POWER FOR HARMONIC. ( 2 )
C
C   NTES - NON-ZERO REQUIRES SUCCEEDING POINTS TO SURROUND
C   INTERPOLATION POINT. ( USE THIS )
C
C   NSMO - 1 SUPPRESSES DEPTH SMOOTHING. ( DON'T SUPPRESS )
C
C88 CARD R(1),R(2),R(3),YINFIN,AINFIN,XOINF,YOINF,INFXI,INFETA
C   - FORMAT(7F10.0,2I5)
C
C   R(1) - SOR ACCELERATION PARAMETER FOR INITIAL GRID.
C   (ZERO VALUE CAUSES VARIABLE ACCELERATION PARAMETER)
C   (FIELD TO BE CALCULATED INTERNALLY)
C   (NEGATIVE VALUE GIVES ALGEBRAIC SYSTEM)
C
C   R(2) - ALLOWABLE X ITERATION ERROR.
C
C   R(3) - ALLOWABLE Y ITERATION ERROR.
C
C   YINFIN - RADIUS OF CIRCULAR OUTER BOUNDARY.
C
C   AINFIN - ANGLE OF FIRST POINT ON CIRCULAR OUTER BOUNDARY (DEGRE

```


C XX
C X THE FOLLOWING, MARKED WITH X, IS FOR ATTRACTION TO COORDINATE LINES/PO
C X
C XX CARD : ATYP,ITYP,MLN,NPT,DEC,AMPFAC - FORMAT(A8,I2,2I5,2F10.0)
C X
C ATYP - TYPE OF ATTRACTION. (XI FOR XI-LINE ATTRACTION,
C ETA FOR ETA-LINE ATTRACTION.) LEFT JUSTIFIED.
C X
C ITYP - ZERO GIVES ATTRACTION ON BOTH SIDES.
C NON-ZERO GIVES ATTRACTION ON UPPER SIDE AND
C REPULSION ON LOWER SIDE.
C X
C MLN - NUMBER OF ATTRACTION LINES.
C X
C NPT - NUMBER OF ATTRACTION POINTS.
C X
C DEC - NON-ZERO DEC USES DEC FOR DECAY FACTOR.
C X
C AMPFAC - NON-ZERO AMPFAC MULTIPLIES ALL AMPLITUDES BY AMPFAC.
C X
C XX CARDS(MLN) : JLM,ALN,DLM - FORMAT(5X,I5,2F10.0)
C (XMIT IF MLN IS ZERO)
C X
C JLM - ATTRACTION LINE INDEX.
C X
C ALN - AMPLITUDE (NEGATIVE REPELS) FOR LINE ATTRACTION.
C X
C DLM - DECAY FACTOR FOR LINE ATTRACTION.
C X
C XX CARDS(NPT) : IPT,JPT,APT,DPT - FORMAT(2I5,2F10.0)
C (XMIT IF NPT IS ZERO)
C X
C IPT,JPT - ATTRACTION POINT INDICES.
C X
C APT - AMPLITUDE (NEGATIVE REPELS) FOR POINT ATTRACTION.
C X
C DPT - DECAY FACTOR FOR POINT ATTRACTION.
C X
C XX
C X THE FOLLOWING, MARKED WITH X, IS FOR ATTRACTION TO SPACE LINES/POINTS
C X
C XX THE FOLLOWING CARDS ARE FOR ATTRACTION TO LINES AND/OR POINTS
C DEFINED BY X,Y COORDINATES. IF MLN IS NOT ZERO, THEN NLM
C OF THE CARDS GIVING NP MUST APPEAR. EACH OF THESE CARDS IS
C FOLLOWED BY NP OF THE CARDS GIVING XPT, ETC. IF NPT IS NOT
C ZERO, THEN NPT OF THE CARDS GIVING XPT, ETC. MUST FOLLOW
C THE LAST GROUP OF THESE CARDS.
C ANY SET NOT WANTED IS REPLACED BY ONE BLANK CARD.
C X
C XX CARD : ATYP,ITYP,MLN,NPT,DEC,AMPFAC - FORMAT(A8,I2,2I5,2F10.0)
C X
C ATYP - TYPE OF ATTRACTION. (XI FOR XI-LINE ATTRACTION,
C ETA FOR ETA-LINE ATTRACTION.) LEFT JUSTIFIED.
C X
C ITYP - ZERO GIVES ATTRACTION ON BOTH SIDES.
C NON-ZERO GIVES ATTRACTION ON UPPER SIDE AND
C REPULSION ON LOWER SIDE.

C 26 NLM - NUMBER OF ATTRACTION LINES.
C 27
C 28 NPT - NUMBER OF ATTRACTION POINTS.
C 29 (NOT INCLUDING POINTS ON ATTRACTION LINES)
C 30
C 31 DEC - NON-ZERO DEC USES DEC FOR DECAY FACTOR.
C 32
C 33 AMPFAC - NON-ZERO AMPFAC MULTIPLIES ALL AMPLITUDES BY AMPFAC.
C 34
C 35 *** CARD : NP - FORMAT(15)
C 36
C 37 NP - NUMBER OF POINTS ON THIS ATTRACTION LINE.
C 38
C 39 *** CARDS : XPT,YPT,APT,DPT,VEC1,VEC2 - FORMAT(6F10.0)
C 40
C 41 XPT,YPT - COORDINATES OF ATTRACTION POINT OR
C 42 POINT ON ATTRACTION LINE.
C 43
C 44 APT - ATTRACTION AMPLITUDE (NEGATIVE REPELS).
C 45
C 46 DPT - DECAY FACTOR.
C 47
C 48 UEC1,VEC2 - X,Y COMPONENTS OF UNIT VECTOR NORMAL TO
C 49 ATTRACTION DIRECTION FOR POINT ATTRACTION.
C 50 (CALCULATED INTERNALLY FOR LINE ATTRACTION.)
C 51
C 52
C 53
C 54 *** THE LAST COORDINATE SYSTEM CONTROL CARD IS THE FOLLOWING CARD :
C 55
C 56 *** CARD : IFAC,IRIT,EFAC - FORMAT(2I5,F10.0)
C 57
C 58 (CAN BE USED TO AID CONVERGENCE BY CONVERGING FIELD)
C 59 (WITH LESS ATTRACTION FIRST AND USING THIS RESULT)
C 60 (AS THE INITIAL GUESS FOR STRONGER ATTRACTION.)
C 61 (BLANK CARD MUST BE INPUT IF THIS FEATURE IS NOT USED.)
C 62 (STANDARD IS TO NOT USE THIS FEATURE , BUT ITS USE MAY)
C 63 (BE NECESSARY WITH STRONG ATTRACTION.)
C 64
C 65 IFAC - NUMBER OF STEPS IN ADDITION OF INHOMOGENEOUS TERM.
C 66 DOUBLES INHOMOGENEOUS TERM AT EACH STEP.
C 67
C 68 (ZERO CONVERGES WITH FULL ATTRACTION.)
C 69 (1.0 CONVERGES WITH NO ATTRACTION FIRST, THEN)
C 70 (WITH FULL ATTRACTION. 2.0 CONVERGES WITH NO)
C 71 (ATTRACTION FIRST, THEN WITH HALF, THEN WITH FULL.)
C 72 (INCREASE NUMBER OF STEPS IF DIUERGENCE OCCURS.)
C 73
C 74 IRIT - NON-ZERO VALUE CAUSES INHOMOGENEOUS TERM TO BE PRINTED.
C 75
C 76 EFAC - MULTIPLE OF CONVERGENCE CRITERION TO BE USED FOR
C 77 INTERMEDIATE CONVERGENCE BETWEEN ADDITIONS OF
C 78 INHOMOGENEOUS TERM. (TYPICALLY 10.0)
C 79
C 80 *** CARD : LDEP,LDOU,LDOB,LDEPF,LIMP,LCOM,LTES,LSMO - FORMAT(8I5)
C 81
C 82 (THIS CARD ALLOWS A SEPARATE SET OF DEPTH POINTS TO BE INPUT
C 83 TO BE USED FOR INTERPOLATION OF DEPTHS ON THE FINAL GRID TO

BE OUTPUT ALONG WITH THE GRID. THIS IS USEFUL IN THE CASE WHERE ADJUSTED DEPTHS WERE USED FOR THE ADAPTATION WHILE ACTUAL DEPTHS ARE DESIRED FOR USE WITH THE GRID IN FLOW CODES.
INPUT A BLANK CARD HERE IF THE FIRST SET OF DEPTH POINTS IS TO BE USED FOR THE OUTPUT DEPTHS. IN EITHER CASE THE OUTPUT DEPTHS ARE LOCATED AT CELL CENTERS BY AVERAGING THE FOUR SURROUNDING GRID POINT VALUES. THE (I,J) OUTPUT DEPTH IS FOR THE CELL WITH (I,J) AT THE LOWER-LEFT CORNER.)

LDEP - NUMBER OF DEPTH POINTS.
(ZERO FOR NON-ADAPTIVE SYSTEM)

LDOUT - NON-ZERO ADDS OUTER BOUNDARY POINTS TO DEPTH POINT LIST, WITH ZERO DEPTH.
(THIS SHOULD BE USED UNLESS THE INPUT DEPTH POINTS EXTEND TO OR BEYOND THE OUTER BOUNDARY. INPUT DEPTH POINTS THAT ARE COINCIDENT WITH OUTER BOUNDARY POINTS WILL RETAIN THE INPUT DEPTH EVEN WHEN THIS FEATURE IS USED.)

LDOP - 1 PRINTS DEPTH POINTS.

LDEPF - NON-ZERO READS DEPTH POINTS FROM FILE 16.

LIMP - INTERPOLATION TYPE : 0 > HARMONIC - ALL
13 > BILINEAR - 3 POINTS
14 > BILINEAR - 4 POINTS
2 > 2-POINT TAYLOR SERIES
3 > 3-POINT TAYLOR SERIES
4 > 4-POINT TAYLOR SERIES
5 > 5-POINT TAYLOR SERIES
-2 > HARMONIC - 2 POINTS
-3 > HARMONIC - 3 POINTS
-4 > HARMONIC - 4 POINTS
-5 > HARMONIC - 5 POINTS

(BEST ARE 13 , 2 , 3 , -2 , -3)

LCOM - NUMBER OF INTERPOLATION POINT SETS FOR TAYLOR. (4)
POWER FOR HARMONIC. (2)

LTES - NON-ZERO REQUIRES SUCCEEDING POINTS TO SURROUND INTERPOLATION POINT. (USE THIS)

LSMO - 1 SUPPRESSES DEPTH SMOOTHING.

*** CARDS(LDEP) : XDEP,YDEP,DEP - FORMAT(3F10.0)
XDEP,YDEP - X,Y COORDINATES OF DEPTH POINT.
DEP - DEPTH.

* MASS STORAGE FILES :
*
RESTART FILE - READ FROM FILE 14 , WRITTEN ON FILE 15 !
RESTART CAN BE FROM PARTIALLY OR FULLY CONVERGED
INITIAL OR ADAPTIVE GRID.

```
C *  
C * (14) RXI, RETA, U, UL, UU, UFAC, OFAC, DEP, XDEP, YDEP  
C * (14) X, Y, LSLIT, LABEL, IMAX, JMAX  
C * (14) NBDY, NUMB, LB1, LB2, LB3, LTYPE, LPT, XL, XU, YL, YU,  
C * DIMI, DIMJ, DIMP, DIMB, LACC, WACC, NEUOUT, NEUBOD, IT1  
C *  
C * COORDINATE SYSTEM STORAGE FILE - FILE 11 :  
C *  
C * (11) LABEL, IMAX, JMAX  
C * ((LSLIT(I,J), I=1,IMAX), J=1,JMAX)  
C * ((X(I,J), I=1,IMAX), J=1,JMAX)  
C * ((Y(I,J), I=1,IMAX), J=1,JMAX)  
C * ((U(I,J), I=1,IMAX), J=1,JMAX)  
C * (OMITTED IF NDEP=0)  
C * (11) NBDY, NUMB, LB1, LB2, LB3, LTYPE, LPT, XL, XU, YL, YU,  
C * DIMI, DIMJ, DIMP, DIMB  
C *  
C *.....
```

APPENDIX B: CYBERNET JOB STREAMS AND EXAMPLE INPUT
FOR CHESAPEAKE BAY

The following files are defined:

BAYR1 = CDC run stream file.
BAYD1 = File containing (x,y) location and the value of depth points.
One depth point per line.
BAY1 = File containing (x,y) location of boundary points. One point
per line.
RPLOTA = CDC plot run stream.
CSPLOT = Plot code source.
WESCOR = Grid code source.

BAYR1

```
/JOB
JFT1XXX(T10,CM300000,P4)
USER,          .KOE.
CHARGE,
SBULIM,AB-77777.
GET,QUESCOR.
GET,TAPE12=BAYD1.
GET,TAPE16=BAYD2.
GET,TAPE10=BAY1.
QUESCOR.
REPLACE,OUTPUT=OUT.
REPLACE,TAPE15=RESTART.
REPLACE,TAPE11=SOLN.
DAYFILE,DAY.
REPLACE,DAY.
EXIT.
REPLACE,OUTPUT=OUT.
DAYFILE,DAY.
REPLACE,DAY.
/EOR
ADAPTIVE
CHESAPEAKE BAY
 76   28    71   50   2   -1    1    1    0    0    0
   1   39     1   -11
   1   39   39   -12
  39   37     3   -11
   3   4   37   -12
  37   39     4   -11
   4   6   39   -12
  39   37     6   -11
   6   7   37   -12
  37   46     7   -11
   7   5   46   -12
  46   48     5   -11
   5   7   48   -12
  48   50     7   -11
   7   5   50   -12
  50   52     5   -11
   5   7   52   -12
  52   54     7   -11
   7   5   54   -12
  54   57     5   -11
   5   7   57   -12
  57   66     7   -11
   7   5   66   -12
  66   68     5   -11
   5   7   68   -12
  68   76     7   -11
   7   11   76   -12
  76   72     11  -11
  11   12   72   -12
  72   73     12  -11
  12   14   73   -12
  73   64     14  -11
  14   16   64   -12
  64   66     16  -11
  16   18   66   -12
  66   64     18  -11
  18   19   64   -12
  64   66     19  -11
```

19	21	66	-12
66	60	21	-11
21	28	60	-12
60	57	28	-11
28	21	57	-12
57	39	81	-11
21	23	39	-12
39	37	23	-11
23	21	37	-12
37	34	21	-11
21	28	34	-12
34	30	28	-11
28	21	30	-12
30	24	21	-11
21	28	24	-12
24	21	28	-11
28	21	21	-12
21	15	21	-11
21	28	15	-12
15	12	28	-11
28	25	12	-12
12	11	25	-11
25	28	11	-12
11	8	28	-11
28	21	8	-12
8	4	21	-11
21	28	4	-12
4	1	28	-11
28	11	1	-12
11	1	1	-12
31	33	6	-1
6	7	33	-2
33	31	7	-1
7	6	31	-2
0	0	0	0
98	1	0	1
1.0	0.001	0.001	13
1.0	1.0	1.0	1.0
1.0	1.0	1.0	1.0

98 1 0 1 13 1 1 0
 /EOF

BAYD1

4.9	6.9	
6.0	6.6	
10.0	8.8	
10.0	8.0	
13.0	8.7	
13.0	7.8	
16.0	8.1	
16.0	7.2	
19.0	9.8	
19.0	8.0	
22.0	10.5	
22.0	9.3	
25.0	10.0	
25.0	8.8	
28.0	10.8	
28.0	9.8	
31.0	11.4	
31.0	10.0	
34.0	12.4	
34.0	11.4	
37.0	13.3	
37.0	12.4	
40.0	14.2	
40.0	13.4	
43.0	14.1	
43.0	13.5	
46.0	13.9	
46.0	13.2	
49.0	13.2	
49.0	12.5	
52.0	12.2	
52.0	11.8	
55.0	10.6	
55.0	10.2	
5.5	6.8	100.0
8.0	8.3	100.0
10.0	8.4	100.0
13.0	8.3	100.0
16.0	7.6	100.0
19.0	8.9	100.0
22.0	9.9	100.0
25.0	9.4	100.0
28.0	10.3	100.0
31.0	10.7	100.0
34.0	11.9	100.0
37.0	12.8	100.0
40.0	13.8	100.0
43.0	13.8	100.0
46.0	13.6	100.0
49.0	12.8	100.0
52.0	12.0	100.0
55.0	10.4	100.0
4.6	6.8	
5.9	6.1	
5.0	6.55	100.0
5.5	6.3	100.0
16.7	7.7	100.0
17.6	7.8	100.0
18.4	8.3	100.0
18.8	8.8	100.0

19.4	9.3	100.0
20.0	9.5	100.0
20.5	9.7	100.0
17.0	7.1	
16.5	8.2	
17.9	7.2	
17.3	8.6	
18.7	7.6	
17.9	8.9	
19.3	8.2	
18.4	9.3	
19.8	8.7	
19.0	9.7	
20.2	9.1	
19.7	10.0	
20.6	9.2	
20.4	10.2	
60.9	4.0	
61.0	4.1	
60.95	4.05	100.0
59.0	6.0	
59.1	6.1	
59.05	6.05	100.0
58.0	6.95	
58.1	7.05	
58.05	7.0	100.0
57.2	8.2	
57.4	8.3	
57.3	8.25	100.0
56.2	9.6	
56.3	9.8	
56.25	9.7	100.0
6.5	7.0	
5.8	8.0	
6.2	7.5	100.0
7.8	7.7	
7.3	8.8	
7.5	8.3	100.0

BAY1

7.8	5.1
7.9	5.3
8.0	5.45
8.15	5.05
8.25	5.75
8.4	5.9
8.6	6.0
8.8	6.1
9.0	6.2
9.3	6.4
9.6	6.6
10.1	6.8
10.9	6.8
11.5	6.9
12.0	6.9
12.7	6.8
13.4	6.4
14.2	6.8
15.0	6.2
15.6	6.9
16.5	5.8
17.1	5.6
17.8	5.5
18.5	6.2
19.5	4.6
21.0	3.7
22.5	2.7
24.0	2.2
25.0	2.6
25.9	3.2
26.6	3.6
27.4	3.8
28.2	3.9
29.5	4.0
30.5	4.8
31.5	5.1
33.0	5.0
33.9	4.7
34.6	4.8
34.6	4.2
34.8	4.4
34.8	4.8
34.8	4.8
34.8	5.3
33.1	5.5
33.1	5.5
32.8	6.2
32.8	6.2
33.9	6.5
35.0	6.1
35.0	6.1
35.2	6.4
35.6	6.7
36.0	6.7
34.0	7.4
38.7	7.2
38.7	7.2
38.9	8.2
38.9	8.2
34.3	9.4

P 60	
34.3	8.4
35.1	10.3
35.9	11.4
36.6	11.6
37.2	12.1
38.0	11.8
38.7	11.3
39.6	11.8
40.3	11.1
40.3	11.1
40.6	10.1
41.1	9.1
41.1	9.1
42.0	9.6
42.7	10.6
42.7	10.6
42.9	11.4
42.9	12.1
42.9	12.1
44.3	12.0
45.0	11.7
45.0	11.7
45.1	10.6
44.9	9.8
44.9	9.8
46.5	9.8
47.8	10.1
47.8	10.1
47.7	11.1
46.7	12.3
46.7	12.3
48.0	12.5
49.2	11.6
49.2	11.6
49.7	10.8
49.8	9.5
49.8	9.5
50.0	9.5
51.4	10.0
52.3	10.3
52.3	10.3
52.4	10.6
52.5	11.0
52.6	11.0
53.1	10.9
53.6	10.6
54.1	10.5
54.6	10.1
55.2	9.8
55.3	9.5
56.3	9.1
56.7	8.6
57.35	7.9
57.36	7.9
57.8	7.1
57.1	6.5
57.1	6.5
57.3	6.3
57.5	6.2
57.5	6.2
??	

P 69	
57.5	6.2
57.55	6.6
57.7	7.0
57.7	7.0
58.1	6.8
58.5	6.8
58.9	5.8
59.2	5.6
59.5	5.3
59.8	4.5
60.8	3.9
61.5	3.4
61.5	3.4
61.6	3.44
61.65	3.48
61.7	3.52
61.7	3.52
61.7	3.52
61.8	4.8
60.2	5.0
59.8	5.5
59.55	5.9
59.55	5.9
59.8	6.2
59.8	6.2
60.8	5.7
60.8	5.7
61.1	6.2
61.3	7.0
61.3	7.0
60.9	7.8
60.4	8.1
59.9	8.2
59.1	8.0
58.5	8.1
58.2	8.5
58.0	9.0
57.4	9.4
56.72	10.0
56.72	10.0
56.7	10.2
56.7	10.4
56.7	10.4
57.6	10.6
58.5	10.2
58.5	10.2
58.52	10.4
58.55	10.6
58.55	10.6
57.6	10.9
56.3	11.1
56.3	11.1
56.3	11.5
56.3	11.5
57.0	11.5
57.5	11.6
57.5	11.6
57.6	11.9
57.5	12.2
57.5	12.2
??	

P 60	
57.5	12.8
57.0	12.8
56.4	12.9
56.0	12.5
55.5	12.8
55.0	13.1
54.1	13.2
54.1	13.2
53.7	14.1
53.6	14.5
53.7	14.9
54.1	15.0
54.3	15.3
54.6	15.6
54.85	15.8
54.85	15.8
54.8	15.9
54.7	16.1
54.6	16.2
54.6	16.2
54.3	16.6
53.8	15.9
53.5	15.6
53.1	15.4
52.8	15.1
52.6	14.7
52.2	14.0
52.2	14.0
51.3	13.7
50.5	13.6
49.3	13.9
48.3	14.7
46.9	15.1
46.8	15.3
46.1	15.2
44.3	15.6
42.8	15.6
41.4	15.5
40.3	15.3
39.6	15.3
38.8	15.2
38.1	15.1
37.6	14.6
36.6	14.0
35.9	13.5
35.0	13.2
36.0	13.2
34.7	13.9
34.4	14.3
34.4	14.3
34.1	14.4
33.6	14.3
33.6	14.3
33.7	13.9
33.8	13.4
33.8	13.4
32.0	13.2
28.8	12.3
28.8	12.3
??	

P .99	
23.8	12.3
23.8	12.7
29.4	13.4
30.1	14.3
30.8	15.3
31.1	16.0
32.2	17.3
32.5	18.2
32.5	18.2
32.6	18.36
31.4	18.5
31.0	18.6
30.6	18.7
30.5	18.8
30.2	17.8
29.6	16.9
28.8	15.8
27.9	15.3
27.0	14.4
26.0	12.4
25.0	11.3
25.0	11.3
23.8	11.2
22.8	11.8
21.8	11.9
21.0	11.8
19.8	11.9
18.7	11.6
18.7	11.6
18.8	13.0
19.0	13.3
19.3	13.7
19.9	14.8
19.7	15.4
20.0	15.8
21.1	16.1
21.1	16.1
21.0	16.4
20.85	16.65
20.7	16.8
20.7	16.8
19.5	16.4
18.8	15.9
18.7	14.9
18.7	14.3
18.1	13.7
17.8	13.1
17.6	11.8
17.6	11.8
16.6	11.4
15.7	11.1
14.9	10.9
14.1	10.8
13.8	11.0
12.3	11.2
12.3	11.2
12.4	11.6
12.6	11.9
12.9	12.1
13.2	12.4
??	

P 60	
13.8	12.4
13.4	12.6
13.7	13.0
13.9	13.3
13.9	13.3
13.7	13.6
13.6	13.8
13.3	14.1
13.3	14.1
12.9	13.7
12.9	13.3
11.8	13.0
11.8	13.0
11.4	13.0
11.4	13.0
11.2	13.7
10.9	14.3
10.9	14.7
10.9	14.7
10.7	14.8
10.45	14.85
10.3	14.9
10.3	14.9
10.2	14.4
10.3	13.9
10.0	13.5
9.4	13.0
8.8	12.4
8.4	11.8
7.7	11.3
7.7	11.3
7.1	11.4
6.6	11.5
6.1	11.7
5.6	11.8
5.6	11.8
5.6	12.6
5.1	13.5
5.4	14.2
6.2	14.7
6.7	15.3
7.1	15.9
7.5	16.5
7.5	16.5
7.2	16.7
6.85	17.0
6.5	17.3
6.5	17.3
6.0	16.5
6.3	15.8
4.9	15.2
3.8	14.6
3.4	13.8
3.2	12.9
3.8	12.0
4.2	11.5
4.3	11.0
4.3	10.5
4.1	10.0
4.0	9.5
??	

	60
4.0	9.5
3.9	9.0
3.6	8.4
3.63	7.9
3.9	7.4
4.1	7.1
4.1	7.1
4.36	6.9
4.6	6.8
5.0	6.55
5.5	6.3
5.9	6.1
5.4	5.8
5.8	5.6
7.3	5.36
7.5	5.8
7.8	5.1
26.0	5.5
27.0	6.3
27.8	6.6
27.8	6.6
27.8	7.4
27.8	7.4
26.9	7.5
26.0	7.4
26.0	7.4
26.0	6.5

RPLOTA

```
'JOB
BHJ1XXX(CM377700,T10,P4)
USER.          ,KOE.
CHARGE,
GET,GCS,OLD=OCS PLOT,OPLTFIL.
COPYL,OLD,OPLTFIL,OCS PLOT,,AR.
REWIND,OCS PLOT.
GET,TAPE10=SOLN.
RFL,140000.
CALL,GCS(I=OCS PLOT,DEV=GCST41)
REPLACE,TAPE66=PLOTCS.
DAYFILE,DAY.
REPLACE,DAY.
EXIT.
REPLACE,OUTPUT=BADOUT.
DAYFILE,DAY.
REPLACE,DAY.
/EOR
      0      0      0      0
      0      0      0      0
11.0      8.0
/EOF
```

As can be seen, the day file from both a grid generation run as well as a run to generate a coordinate plot is stored in a permanent file called DAY. Printed output from a grid run is stored in a permanent file called OUT. The following sequence of commands would be issued from a Tektronix terminal to first run the grid model, then run the plot code, and finally to plot the boundary-fitted coordinate system on the screen.

```
GET,BAYR1 - Creates a local file called BAYR1 from the permanent
file BAYR1.

SUBMIT,BAYR1 - Run stream BAYR1 is submitted as a batch job.

XEDIT,DAY,P - Look at day file to see if the grid run was successful.

XEDIT,OUT,P - Look at the printed output from the grid run.

GET,RPLOTA - Creates a local file called RPLOTA from the permanent
file RPLOTA.

SUBMIT,RPLOTA - Run stream RPLOTA is submitted as a batch job.

XEDIT,DAY,P - Look at day file to see if the plot run was successful.

OLD,PLOTCS { - Coordinate system is plotted on the screen
LHN }
```

E

N

D

I

TIC

8-

86